

# University of Cincinnati

Date: 11/7/2022

I, JT Toebe, hereby submit this original work as part of the requirements for the degree of Master of Science in Toxicology (Environmental Health).

It is entitled:

**Carnosine-treated mice exhibit DNA methylation changes in Parkinson's disease-related genes and biological processes**

Student's name: JT Toebe

This work and its defense approved by:

Committee chair: Mary Beth Genter, Ph.D.

Committee member: Katherine Burns, Ph.D.



44225

# **Carnosine-treated mice exhibit DNA methylation changes in Parkinson's disease-related genes and biological processes**

A thesis submitted to the  
Graduate School  
of the University of Cincinnati  
in partial fulfillment of the  
requirements for the degree of

Master of Science

in the Department of Environmental and Public Health Sciences  
of the College of Medicine

by

JT Toebbe

B.S. Murray State University

May 2019

Committee Chair: Mary Beth Genter, Ph.D., D.A.B.T., A.T.S.

# Abstract

Parkinson's disease (PD) is an increasingly prevalent neurodegenerative disease in our society that presents with devastating symptoms that are mainly characterized by progressive motor deficits. A single cause of PD has not yet been elucidated, but the most supported etiology is the aggregation of alpha synuclein (aSyn), a protein found throughout the nervous system. Harmful aggregates form in the substantia nigra (SN), affecting the production of dopamine and prompting the loss of motor function. Oxidative stress and post-translational modifications of the protein may promote formation of aSyn aggregates, as well as environmental and genetic factors.

Current therapeutics for PD lack the ability to modify disease progression and are not ubiquitously effective, so more focus on developing a treatment is required. In the Genter Laboratory, intranasal (IN) administration of carnosine was shown to decrease aSyn in both the olfactory epithelium (OE) and the SN in a mouse model of PD. Carnosine is a naturally-occurring dipeptide that has metal chelating and anti-oxidative stress, as well as improving clinical outcomes for PD patients prescribed oral carnosine in addition to the standard of care.

To understand the basis for the beneficial effects of carnosine in decreasing aSyn aggregation in the OE in mice, reduced representation bisulfite sequencing (RRBS) DNA methylation analysis was performed to identify potential epigenetic changes resulting from IN carnosine treatment. We tested the hypothesis that the observed decreased of aSyn in the OE is due to methylation differences in the promoter of aSyn or other genes related to PD. In the analysis, differentially methylated genes were evaluated for their relevance to PD, and reverse transcription-quantitative polymerase chain reactions (RT-qPCR) and immunostaining were used to further evaluate effects of differential methylation.

Analysis of differentially methylated genes revealed that the methylation status of the aSyn promoter was unaffected by carnosine, indicating that decreased accumulation is not a result of hypermethylation and subsequent silencing of the aSyn gene. Other genes related to PD with differentially methylated promoters included discoidin domain receptor tyrosine kinase 1 (*Ddr1*), G-protein coupled receptor 4 (*Gpr4*), DnaJ homolog C 6 (*Dnajc6*), and copper metabolism MURR1 domain protein 1 (*Commd1*). The *Ddr1* promoter was hypermethylated, while the *Gpr4*, *Dnajc6*, and *Commd1* promoters were hypomethylated after carnosine treatment. Further functional enrichment analysis of the RRBS data using ToppGene showed that several neuro-based biological processes were affected in mice IN carnosine treatment, such as neuron development and neurogenesis. These results show that IN carnosine treatment does not alter aSyn aggregation via epigenetic alterations; however, other genes and canonical pathways related to neurological function are differentially methylated, signifying potential mechanism for carnosine's beneficial effect on PD in mice and humans.

Copyrighted by

JT Toebbe

2022

## Acknowledgements

First, I want to express the most appreciation for Dr. Mary Beth Genter and everything she has done for me over the past couple of years. Not only has her lab provided me with a place to develop skills that are crucial to my future, but she has helped me grow as a person. I have had the opportunity to take on responsibilities, which has allowed my confidence and self-esteem to blossom. Her door was always open to me, and we were able to discuss whatever was on my mind, which was extremely helpful for me as I went through the struggles of being a graduate student. For this, I am incredibly grateful.

I would also like to thank Dr. Katherine Burns for her contributions as a member of my committee, as she was an integral part of developing my thesis. She has provided great insight and has been extremely gracious with her time, despite her schedule, which I know can be hectic. I also want to thank her for everything she taught me during my rotation in her lab. From lab techniques to the mindset of a graduate student, I will move forward knowing that the experiences I had in her lab helped me grow into the scientist I am now.

Within the Department of Environmental and Public Health Sciences, I would like to thank Dr. Divaker Choubey for allowing us to use his reagents and antibodies that helped us to progress this project. Also, the other students in the Toxicology program were all great to talk to about any problems I had or anything I needed in my research. Taylor Wilson was always an outlet for me to talk to from the time we worked together in Dr. Burns' lab and throughout my time in Dr. Genter's lab. Paul Deford played a big role in my research progress when he offered me his senior advice as an elder student in the program. He provided me with any information I needed to succeed in the lab and in presentations, specifically our program seminar.

Thank you to John Snowball at Cincinnati Children's Hospital, who helped show us how to use TopoFun for functional enrichment analysis with our methylation data.

I would like to thank my family. My parents have always supported my education, and my interest in science. None of this would have been possible without them. My brother, Ben, has been an outlet for me to talk about my interests in biology and science for years, which has been so important to my critical thinking and passion for learning. Lastly, Kourtney, my wife, has had the pleasure of experiencing the trials and tribulations of graduate school through my time at the University of Cincinnati. She puts so much effort into being the amazing elementary teacher that she is, but that never detracted from her being my biggest supporter. Throughout my graduate studies, my family has been there to listen to my presentations or read my papers. For this, I am eternally grateful.

# Table of Contents

Abstract.....	ii
Acknowledgements.....	v
Table of Contents.....	vii
List of Tables.....	x
List of Figures.....	xi
Introduction.....	1
Parkinson's Disease.....	1
Environmental Factors and PD.....	1
Genetic Factors and PD.....	2
Alpha Synuclein (aSyn) Pathology.....	4
Current Therapeutics.....	4
Carnosine.....	6
Hypothesis.....	9
DNA Methylation and Follow-up Analyses.....	10
Rationale for DNA Methylation Analysis.....	10
Methods.....	11
Mice and Treatment.....	11

Reduced Representation Bisulfite Sequencing and Analysis.....	12
Differential Methylation Screening.....	13
Pathway Analysis.....	14
mRNA Transcript Expression.....	14
Immunostaining/Confocal Microscopy.....	15
Copper (II) Chelation.....	19
Results.....	20
Methylation Data Analysis of <i>Snca</i> and Other Genes.....	20
RT-qPCR.....	26
Immunostaining.....	27
Copper (II) Chelation.....	33
Pathway Analysis.....	34
Discussion.....	36
RRBS and Methylation of PD-related Genes.....	36
mRNA Expression.....	39
Immunostaining.....	40
Copper (II) Chelation.....	42
Pathway Analysis.....	42

Future Directions.....	43
Conclusions.....	45
Bibliography.....	47

## **List of Tables**

Table 1. Primers used for real time PCR analysis.....	15
Table 2. Location and methylation status of restriction fragments and their associated genes...	21

## List of Figures

Figure 1. Carnosine Structure.....	7
Figure 2. Diagram of differential methylation calculation and selection of genes of interest.....	14
Figure 3. Alignment of Ddr1, Gpr4, Dnajc6, and Commd1 fragments displays differential methylation profile exhibited by carnosine treatment.....	25
Figure 4. RT-qPCR analysis portrays expression differences for Ddr1 and Gpr4 following carnosine treatment, not Snca.....	26
Figure 5. Immunohistochemistry staining suggests DDR1 localization to olfactory neurons and nerve bundles in the olfactory mucosa.....	27
Figure 6. Immunofluorescent co-localization with OMP confirms the presence of DDR1 in olfactory neurons and nerve bundles.....	28
Figure 7. DDR1 protein level was unchanged in carnosine-treated mice.....	29
Figure 8. Immunofluorescent co-localization shows absence of GPR4 in neurons and presence in the ducts of Bowman’s glands in the mouse olfactory epithelium.....	31
Figure 9. Immunohistochemistry staining shows the presence of DNAJC6 in the nerve bundles and along the surface of the olfactory epithelium.....	32
Figure 10. Immunohistochemistry staining shows the presence of COMMD1 in the sustentacular cells and ducts of Bowman’s glands in the olfactory mucosa.....	33
Figure 11. Assessment of carnosine-Cu <sup>2+</sup> complex formation using absorbance confirms carnosine’s ability to chelate copper.....	34

Figure 12. Pathway analysis network map displays trend of neurological pathways affected by differential methylation in carnosine-treated mice.....35

# Introduction

## **Parkinson's Disease: Background**

Parkinson's disease (PD) afflicts nearly 10 million people across the globe, with about 1% of the population over 60 years of age affected by the condition (Vidović and Rikalovic 2022; de Lau and Breteler 2006). Despite the pervasiveness of PD in our society, there is still an absence in understanding the mechanisms or causes of disease development and progression. Age is the most strongly related factor; as age increases so does the risk of developing the PD. Prevalence can reach upwards of 4% after the age of 80 (de Lau and Breteler 2006). After that age, there appears to be a gender bias, with men being 1.5 times more likely to develop PD than women (Wooten et al. 2004).

In the brains of PD patients, neurodegeneration most prominently affects the substantia nigra (SN), a region of the midbrain that is part of basal ganglia (Fearnley and Lees 1991; Bolam et al. 2009). Neurons in the SN pars compacta region produce the neurotransmitter dopamine, which is used by neurons in the striatum to control motor function (Damier et al 1999; Nicola et al. 2000). Loss of these neurons is associated with PD and the characteristic motor deficits observed in patients (Kalia and Lang 2015).

## ***Environmental Factors and PD***

In addition to age, environmental and genetic factors may also play a role in PD development. Throughout life, humans have an intimate relationship with their surroundings, ingesting, inhaling, and absorbing many substances. Exposure to environmental chemicals, such as pesticides, has long been associated with increased risk of PD. This association began with the discovery of 1-methyl-4-phenyl-1,2,3,6-tetrahydropyridine (MPTP). In 1982, several individuals

displayed symptoms similar to PD after using a synthetic heroin containing MPTP (Langston et al. 1983). The pure parkinsonism characteristics of these patients suggested that MPTP, a lipophilic molecule that can cross the blood brain barrier, was selectively targeting the dopaminergic neurons of the substantia nigra pars compacta. In the brain, MPTP is converted to MPP<sup>+</sup>, which is the toxic metabolite that is selectively taken up by dopaminergic neurons of the SN (Langston et al. 1984; Shen et al. 1985). The toxicity of MPP<sup>+</sup> stems from its ability to utilize the dopamine transporter to enter neurons and, subsequently, concentrate in the mitochondria, where it inhibits complex I of the electron transport chain (Kopin 1987). Paraquat, a structural analog of MPP<sup>+</sup>, is used as a pesticide, and epidemiological studies have identified occupational pesticide exposure as a risk factor for neurodegeneration (Islam et al 2021).

### ***Genetic Factors and PD***

From a genetic viewpoint, familial PD accounts for approximately 5-10% of all PD cases (Bostantjopoulou and Fidani 2016). Once thought to be a non-genetic “sporadic” disease, several genes are now associated to monogenic forms of PD, including alpha synuclein (*SNCA*), *DJ-1*, parkin (*PRKN*), and leucine-rich repeat kinase 2 (*LRRK2*) (Gasser 2009; Lesage and Brice 2008). Gene-associated risk factors are all linked with mutations within gene loci, such as insertions, deletions, and point mutations. In the case of *SNCA*, there are six known point mutations (A53T, A30P, E46K, H50Q, G51D, and A53E), along with examples of gene duplications and triplications (Brás and Outeiro 2021).

Epigenetic changes may also impact an individual’s risk of developing PD. The most common epigenetic change is DNA methylation, where DNA methyltransferases enzymes covalently add methyl groups to cytosine residues in regions of DNA rich in cytosine and guanine, also known as CpG islands (Qureshi and Mehler 2011). When highly methylated

regions of DNA are located in regulatory regions near the transcription start sites, such as promoters, transcript expression of the respective gene is predicted to be repressed. A gene with a hypomethylated promoter is expected to have increased expression. In the context of PD, the *SNCA* gene region contains two CpG islands: one in the first exon and another in the first intron (Matsumoto et al. 2010). Methylation of the intronic CpG island repressed *SNCA* expression. However, the transcript was overexpressed when the cells were treated with a DNA methylation inhibitor, signifying the influence of this CpG island on the regulation of *SNCA* expression. This finding coincides with the observed methylation status of the intronic CpG island in the SN of post-mortem PD patients (Matsumoto et al. 2010).

In addition to *SNCA*, other PD-associated genes have been observed to have altered methylation of regulatory regions. *PRKN*, or the *PARK2* locus, is the most commonly mutated gene in autosomal recessive juvenile parkinsonism and is also considered a risk factor for early-onset PD (EOPD) (Lücking et al. 2000). The promoter of *PRKN* is shown to be hypomethylated in patients diagnosed with EOPD (Eryilmaz et al. 2017).

While genetic and environmental factors certainly play a role in increasing likelihood of developing PD, a single mutation or exposure might be necessary, yet it is not likely to be sufficient (Dardiotis et al. 2013). For example, PTEN-induced kinase 1 (PINK1) is a protein that localizes to the mitochondria and protects neurons against oxidative stress and mitochondrial dysfunction. *PINK1* gene mutations leading to decreased function are linked to EOPD development (Valente et al. 2004). An individual with a mutated *PINK1* might not develop PD, but exposure to an environmental insult that specifically attacks mitochondrial function, such as rotenone, may further increase that risk.

### ***Alpha Synuclein (aSyn) Pathology***

aSyn is a small, flexible protein that is commonly found near presynaptic terminals and the nuclear envelope in neurons (Maroteaux et al. 1988). In both sporadic and familial PD patients, aSyn aggregates are commonly present and enable the formation of Lewy bodies in neurons of the SN (Spillatini et al. 1998). Genetic mutations and duplication events can lead to increased risk of aSyn oligomerization and have been implicated in autosomal dominant forms of PD (Brás and Outeiro 2021).

With or without mutations, post-translational modifications (PTMs) on aSyn may favor the aggregated form. When acetylated at the N-terminus, aSyn showed a propensity to remain in a helical conformation, which is less prone to aggregation when compared to a  $\beta$ -sheet structure (Bartels et al. 2014; Chen et al. 2015). Also, phosphorylation and dephosphorylation of serine (Ser) and tyrosine (Tyr) residues, are associated with an increased risk of oligomer formation (Fujiwara et al. 2002; Chen et al. 2009). Ser129 and Tyr125, two frequently phosphorylated residues in aSyn, do not appear to be selectively modified by one specific kinase or phosphatase, but pololike kinase 2 (PLK2) and the Src protein-tyrosine kinase family play a role in phosphorylating Ser129 and Tyr125, respectively, promoting conformational changes within the protein (Inglis et al. 2009; Ellis et al. 2001). Pharmacologically targeting kinase activity that impacts aSyn conformation could be an avenue to explore for future interventions for PD.

### **Current Therapeutics to Treat PD**

PD is a slowly-progressing disease that develops over time. Prior to the loss of motor function, which is the most well-known presentation of PD, other symptoms develop that signify the onset of the disease, such as olfactory dysfunction, cognitive impairment, and sleep disorders

(Khoo et al. 2013). These early symptoms characterize the prodromal stage of PD. As the disease progresses, dyskinesia and psychosis become more prominent. These physical detriments are accompanied by autonomic symptoms, such as urinary incontinence and/or constipation (Kalia and Lang 2015).

To date, pharmacological interventions are limited to treating the clinical symptoms, rather than trying to slow or stop disease progression (Kalia and Lang 2015). Several strategies have been used to lessen symptoms and improve quality of life with the disease by targeting the observed decrease of dopamine and dopaminergic neurons in the SN: replacing dopamine supply, increasing receptor sensitivity to dopamine, and inhibiting dopamine breakdown (Ellis and Fell 2017). To increase the amount of dopamine available in the synaptic cleft, a dopamine precursor, such as Levodopa (L-DOPA), is administered, which undergoes bioactivation to form dopamine. L-DOPA is currently the standard of care for PD treatment but is known to lose efficacy as the total time of treatment lengthens. In a cumulative study of dyskinesias in PD patients, almost 40% of individuals started displaying symptoms after 4-6 years of treatment. That number increased to 90% in trials lasting at least 9 years (Ahlskog and Muentner 2001).

To counteract the loss of efficacy in L-DOPA treatment, combination therapies have been trialed with several drugs with various mechanisms. To increase dopamine's impact on neurons, dopamine receptor agonists, such as apomorphine, act on one of the five dopamine receptors (D<sub>1</sub>-D<sub>5</sub>) (Ellis and Fell 2017). Apomorphine, which can be administered through subcutaneous injection or inhalation, has been shown to significantly improve PD patient motor function in conjunction with L-DOPA (Deleu et al. 2004; Grosset et al. 2014). To increase dopamine concentration by inhibiting its breakdown, potent inhibitors of monoamine oxidase B (MAO-B) are utilized, such as selegiline. MAO-B is responsible for transforming dopamine to 3,4-

dihydroxyphenylacetic acid, which is eventually converted to homovanillic acid by catechol-O-methyltransferase (COMT), another putative drug target for PD (Ellis and Fell 2017). Selegiline and a related MAO-B inhibitor, rasagiline, are known to possess neuroprotective properties, while only rasagiline showed the potential to rescue neurodegeneration (Zhu et al. 2008).

Both dopamine receptor agonists and MAO-B inhibitors can induce more severe adverse events, so they may not be preferred to L-DOPA, unless the symptom improvement is significant. In a study comparing L-DOPA versus L-DOPA-sparing drugs (dopamine agonists and MAO-B inhibitors), patients given the L-DOPA-sparing drugs were more likely to stop treatment due to adverse events than patients only give L-DOPA, which is generally tolerated well (PD Med Collaborative Group et al. 2014). The adverse events most reported with apomorphine and other dopamine agonists include nausea, vomiting, and confusion/hallucinations (Bhidayasiri et al. 2016; Alonso Cánovas et al. 2014). With MAO-B inhibitors, such as safinamide, patients experienced headache, hypertension, and vomiting (Stocchi et al. 2012; Borgohain et al. 2013).

### **Carnosine**

With the lack of disease-modifying therapies for PD patients, current research efforts are geared towards targeting observed PD pathologies, such as mitochondrial dysfunction and oxidative stress (Winklhofer and Haass 2010; Dias et al. 2013). Mitochondrial function is reported to be a determining factor of ROS production within the cell (Murphy 2009). Generation of ROS, such as superoxide and hydrogen peroxide, occur when ATP production is interrupted. This matches the mechanism of action in the MPTP model of PD, where complex I of the electron transport chain is inhibited (Kopin 1987).

The widely accepted aSyn aggregate pathology is supported by the biological effects of mitochondrial dysfunction and subsequent ROS production. When ROS levels increase within a cell, oxidative damage affects proteins, including aSyn (Paxinou et al. 2001; Scudamore and Ciossek 2018). The same effect was observed when rotenone, a complex I inhibitor, was given to rats subcutaneously (Sherer et al. 2003). Finding a therapeutic candidate that can affect at least one of these mechanisms could be vital to turning around the outlook of PD treatment.

$\beta$ -Alanyl-L-histidine, better known as carnosine (CAS no. 305-84-0), was first identified in muscle at the beginning of the 1900s (Figure 1) (Quinn et al. 1992). Carnosine was also discovered in specific regions of the brain and olfactory system, such as the SN and olfactory bulb (Margolis 1974; Kish et al. 1979). Carnosine localizes to the olfactory bulb via axons of olfactory neurons after intranasal (IN) administration, signifying its potential to be therapeutically available to deeper brain regions post-treatment (Burd et al. 1982). Peptide transporter 2 (Pept2) is responsible for transporting carnosine and is expressed throughout the body, including the olfactory epithelium (OE) (Teuscher et al. 2004; Kamal et al. 2008; Bermúdez et al. 2019).

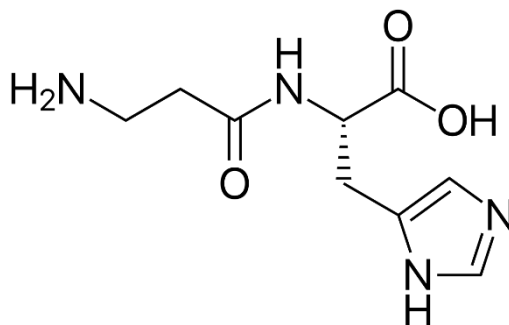


**Figure 1. Carnosine Structure.**

For a pharmacological agent to target neurodegenerative disease pathology, the drug needs to be in an active form in the brain, which is an obstacle in PD therapy development (Stocchi and Olanow 2013). In the case of carnosine, IN, versus oral, administration can avoid drug degradation in the liver or hydrolysis in the serum by carnosinases (Jadhav et al. 2007; Bellia et al. 2014). Interestingly, the expression of cytosolic non-specific dipeptidase 2 (CNDP2), which hydrolyzes carnosine to alanine and histidine, is upregulated in the SN of PD patients (Bellia et al. 2014; Licker et al. 2012).

The most supported mechanism for carnosine action in PD therapy is protection against oxidative stress. Carnosine achieves this in two ways: scavenging ROS and protecting superoxide dismutase (SOD) (Hartman et al. 1990; Pavlov et al. 1993; Choi et al. 1999). Superoxide is a negatively charged free radical ( $O_2^{\bullet-}$ ) that is produced when oxidative phosphorylation in the electron transport chain is interrupted and reducing equivalents, such as NADH, build up inside the mitochondria (Wallace et al. 2010). The superoxide free radical is converted to  $H_2O_2$  by SOD.  $H_2O_2$  can subsequently be reduced to a hydroxyl radical ( $HO^{\bullet}$ ).  $HO^{\bullet}$  damages macromolecules within the cell, including SOD, reducing the capacity to control further ROS production resulting from mitochondrial dysfunction. *In vivo*, carnosine treatment reduced SOD degradation and prolonged the average life span of mice with an ROS imbalance (Stvolinskii et al. 2003).

Mitochondrial function is intertwined with oxidative stress and aSyn in PD etiology, and a mouse model overexpressing aSyn showed decreased expression of complexes I, III, IV, and V in the electron transport chain (Bermúdez et al. 2018). However, IN carnosine treatment in these mice increased expression of complexes I, IV, and V, showing a potential transcription-level effect. Relatedly, the function of complex IV was significantly increased in a mitochondrial

function assay (Bermúdez et 2018). To assess carnosine's effects on the PD phenotype, the same aSyn-overexpressing mouse model was used and IN carnosine treatment prevented the motor decline observed in the vehicle-treated mice in a dose-related manner (Bermúdez et al. 2019; Brown et al., 2021). IN carnosine also decreased aSyn levels in the OE and SN (Bermúdez et al. 2019; Brown et al. 2021).

Carnosine is well tolerated, based on pharmacological studies in rodents (Horisaka et al. 1974; Bae et al. 2013). The LD<sub>50</sub> in mice is 9,087 mg/kg for intraperitoneal administration (Horisaka et al. 1974). In the same study, no effects on the central nervous system were observed below lethal doses. In rats, doses up to 2000 mg/kg per day were well tolerated; no significant changes in body weight or food consumption were observed (Bae et al. 2013). Organ-specific toxicity in rats was evaluated by histopathology, but no effect was observed in the bone marrow, cerebellum, cerebrum, brain stem, hippocampus, heart, lung, liver, or kidney.

In a human trial, carnosine was given to PD patients orally (1.5 g/day) in combination with L-DOPA, the standard of care treatment (Boldyrev et al. 2008). When compared to the standard treatment, the carnosine + L-DOPA group had significantly improved clinical outcomes: rapid hand movement, leg agility, and daily activities. SOD activity in the red blood cells of the carnosine-treated patients also showed significant improvement when compared to the standard treatment, supporting the hypothesis that carnosine acts as an antioxidant (Boldyrev et al. 2008).

### **Hypothesis**

When carnosine was investigated as a potential disease-modifying therapeutic, it showed neuroprotective potential across several etiologies: oxidative stress, mitochondrial function, and

aSyn aggregation. Oligomerization of aSyn is strongly associated with PD, and IN carnosine treatment decreases aSyn levels in the OE and SN *in vivo* (Bermúdez et al. 2019; Brown et al. 2021). This supports the observed improvement in motor function in patients treated with carnosine (Boldyrev et al. 2008). However, the mechanism for the observed aSyn reduction in the OE and SN is not known.

Epigenetic changes have been implicated in increased risk for PD, and *SNCA* has two known CpG islands that can be variably methylated (Qureshi and Mehler 2011; Matsumoto et al. 2010). This project was designed to evaluate epigenetic differences of the *Snca* CpG islands and throughout the whole mouse genome in response to IN carnosine treatment. We hypothesized that the previously observed decrease in aSyn aggregation in the OE and SN is due to methylation differences in regulatory regions of *Snca* or other PD-related genes. To test the hypothesis, reduced representation bisulfite sequencing (RRBS) was performed to evaluate the methylation status of restriction fragments throughout the mouse genome. Differentially methylated genes were evaluated for their relevance to PD. Molecular approaches, such as reverse transcription-quantitative polymerase chain reactions (RT-qPCR) and immunostaining, were used to further evaluate effects of differential methylation.

## **DNA Methylation and Follow-up Analyses**

### **Rationale for DNA Methylation Analysis**

IN carnosine administration in mice was shown to decrease aSyn levels in the OE, but the mechanism behind that decrease was not elucidated (Bermúdez et al. 2019). We hypothesized that epigenetic changes in regulatory regions of the *Snca* gene or other PD-related genes may be associated to that previous observation. To test this hypothesis, mice were treated with 2 mg of

carnosine, intranasally, every day for 8 weeks. Then, reduced representation bisulfite sequencing was used to portray the methylation profiles of potentially regulatory regions of the mouse genome. By comparing the methylation status of genes of the carnosine-treated versus the vehicle-treated mice, we could predict whether a gene's expression could be upregulated or downregulated. This process led to identification of other PD-related genes with epigenetic (DNA methylation) differences after IN carnosine administration. Further analysis of downstream mRNA expression and protein localization allowed us to compare changes in methylation to effective regulation of that respective gene.

## **Methods**

### ***Mice and Treatment***

Wild type BDF-1 mice were bred for use in experiments (Charles River, strain 099) in the University of Cincinnati Laboratory Animal Medical Services vivarium under barrier conditions. At four weeks of age, mice were genotyped, weaned, and randomly assigned to a treatment group. Mice were weaned to lixite polysulfone shoebox cages with corncob bedding and enrichment (nestlet and shredded paper). Mice were housed in an inverted 12-hour light-dark cycle (lights on at 21:00 and out at 09:00). Food and water were provided *ad libitum*, except during food restriction. Starting at 4 weeks of age, 2 mg of carnosine was administered intranasally every day for 8 weeks (Bermúdez et al. 2018; Bermúdez et al. 2019; Brown et al. 2021). IN dosing was approximately 5 uL per nostril, 10 uL total each day. Control mice received an equal volume of ultrapure, sterile water. Carnosine (98%) was supplied by Acros Organics (New Jersey, USA). Carnosine was stored at 4°C and dosing solution was prepared daily. Carnosine was dissolved in ultrapure sterile water at concentrations of 0.20 mg/uL, for a total of 2 mg in 10 uL. Animals were monitored for body weight, mortality, and clinical

symptoms throughout the study. All experiments were conducted under protocols approved by the University of Cincinnati Institutional Animal Care and Use Committee and in full accordance with the 8th Guide for the Care and Use of Laboratory Animals. After 8 weeks of carnosine or vehicle treatment, mice were euthanized with carbon dioxide; the ethmoid turbinates and the caudal one-third of the nasal septum, which are covered with OE, were harvested as previously described and frozen at -70°C (Genter et al. 2003). For immunostaining, mice were euthanized, and nasal cavities were fixed by infiltration with neutral buffered formalin, followed by decalcification in 10% formic acid. Tissues were embedded in paraffin and sectioned.

### ***Reduced Representation Bisulfite Sequencing and Analysis***

Prior to reduced representation bisulfite sequencing (RRBS), DNA was isolated from OE tissue with Qiagen DNeasy Blood and Tissue kit (Qiagen, cat. 69504). The isolated DNA was sent to Active Motif® (Carlsbad, CA, USA). Once received, DNA was digested with restriction enzymes Msp1 and Taq1 to cut C<sup>^</sup>CGG and T<sup>^</sup>CGG sequences, respectively, which ensures CpG islands at the end of the restriction fragments. A-tail adapters were ligated to the fragments for compatibility with Illumina 3'-T adapters. Bisulfite conversion deaminated unmethylated cytosines to form uracil, which were read as thymidine during sequencing. Methylated cytosine remained unchanged. DNA was PCR-amplified prior to sequencing using the Illumina Next-Generation Sequencing platform (San Diego, CA, USA). The sequences alignment was generated by Illumina NextSeq 500, and the information was stored in BAM files. For data visualization, BAM files were loaded into Integrative Genomics Viewer (IGV, Broad Institute) to display methylation patterns of restriction fragments. Quantitative differential methylation data was generated by the DNA methylation analysis package (DMP), and the fragments were

annotated by HOMER, which provided details, such as distance to the transcription start site (TSS) (Stockwell et al. 2014; Heinz et al. 2010).

### ***Differential Methylation Screening***

The goal of screening the RRBS data was to observe differences in methylation of potentially regulatory regions of *Snca* and other genes related to PD. For a fragment to be considered, it had to be located within +/- 1000bp of the TSS for the associated gene. When processing the data, the proportion of a restriction fragment that was methylated for both vehicle-treated and IN carnosine-treated mice was compared. When an absolute difference of 20% hypo/hypermethylation was observed for a gene, it was considered a gene of interest (Figure 2). Previous studies utilized 10-15% differential methylation as a cutoff point when investigating methylation and mRNA expression (Ng et al. 2012; Blake et al. 2020). Differential methylation was visualized in IGV using the BAM files provided by Active Motif (Carlsbad, CA). Subsequently, a literature search was performed for each gene of interest to evaluate previously described relation to PD. The resulting list of genes was considered for further analysis via molecular approaches, such as RT-qPCR and immunostaining.

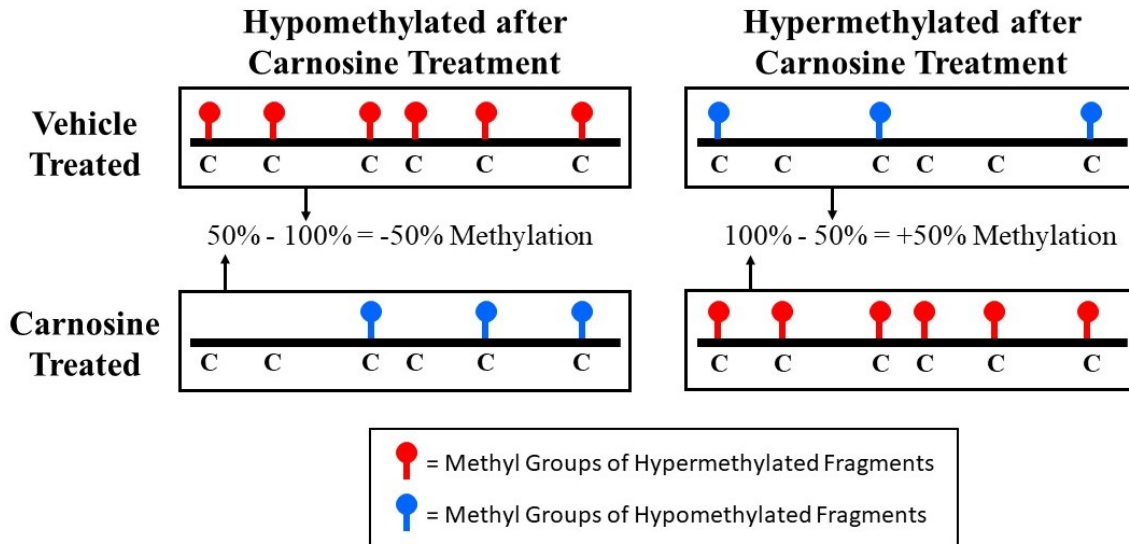


**Figure 2. Diagram of differential methylation calculation and selection of genes of interest.** The percentage methylation of each fragment was provided by the RRBS data. That percentage was compared between both treatment groups.

### *Pathway Analysis*

Functional enrichment analysis was crucial to elucidating pathways that were collectively affected by IN carnosine treatment. We excluded fragments outside of the potentially regulatory range (+/- 1000 bp) and separated them into two categories: hypermethylated vehicle treated mice and hypermethylated IN carnosine treated mice. From each group, a list of gene identifiers (e.g. RefSeq) was inserted into ToppFun (<https://toppgene.cchmc.org/enrichment.jsp>, Cincinnati Children’s Hospital Medical Center), which utilized the list to identify gene ontology (GO) pathways significantly associated with methylation changes in the respective group.

### *mRNA Transcript Expression*

To evaluate how differential methylation affects downstream expression of *Snca* and other genes of interest, we employed reverse transcription-quantitative polymerase chain reaction (RT-qPCR). RNA was isolated from OE tissue stored in RNAlater™ at -20°C using Tri Reagent®

(Molecular Research Center Inc., cat. TR118). The isolated RNA was reverse transcribed with the Verso cDNA synthesis kit (ThermoFisher, cat. AB1453A) and stored at -80°C until needed. Quantitative PCR was performed with the QuantStudio™ 3 Real-Time PCR System (ThermoFisher, Waltham MA, USA). For PCR, Fast SYBR™ Green Master Mix (ThermoFisher, cat. 4385612) was used and supplied protocol was followed. Primers for analyzed genes are found in Table 1 and were produced by Integrated DNA Technologies, Inc. (IDT, Coralville, IA, USA). Cycle threshold (Ct) values of experimental genes were normalized to  $\beta$ -actin (*Actb*) levels to compare expression differences between vehicle and IN carnosine treated mice.

Table 1. Primers used for real time PCR analysis\*

Gene	Gene ID (RefSeq)	Forward Primer (5'→3')	Reverse Primer (3'→5')
<i>Actb</i>	NM_007393.5	AGAGGGAAATCGTGCGTGAC	CAATAGTGATGACCTGGCCGT
<i>Snea</i>	NM_001042451.2	ACAGTGTGTTTCAAAGTCTTCCAT	CTGTAGTGAGAGGGGAGCAC
<i>Ddr1</i>	NM_172962.1	CCCTTTGGGCAGCTTACAGA	GCCTGGACAAGTAGACCTGC
<i>Gpr4</i>	NM_175668.4	AGTCGGGACCAAGTCAGAGA	AGTGGTGGAGCACAGGATTG

\*Primers used for real time PCR analysis were designed using NCBI Primer Blast (Bethesda, MD, USA).

### ***Immunostaining/Confocal Microscopy***

Discoidin Domain Receptor Tyrosine Kinase 1 (DDR1):

For staining, sections (5  $\mu$ m) were dewaxed with CitriSolv (Deacon Labs, cat. 1601) and subsequently hydrated with 95% EtOH, 75% EtOH, and phosphate buffered saline (PBS) plus Tween (10 mM PB, 0.9% saline, 0.1% Tween-20). Antigen retrieval was performed with SignalStain® Citrate Unmasking Solution (Cell Signaling Technology, cat. 14746), where the solution was brought to a boil and kept around 95°C for 10 minutes. The slides in solution were

then cooled for 30 minutes at RT before washing with dH<sub>2</sub>O. Endogenous peroxidase was quenched with 3% hydrogen peroxide, which remained on the slides for 10 minutes at RT. Sections were washed with dH<sub>2</sub>O again. Animal-free blocking solution was added to the slides for 1 hour at RT. Then, sections were incubated with rabbit anti-mouse DDR1 primary antibody (Cell Signaling Technology, cat. 5583) at 1:1000 in SignalStain<sup>®</sup> antibody diluent (Cell Signaling Technology, cat. 8812) overnight at 4°C. After washing with Tris Buffered Saline with Tween (TBST) (Cell Signaling Technology, cat. 9997), SignalStain<sup>®</sup> Boost Detection Reagent (Cell Signaling Technology, cat. 8814), an HRP conjugated anti-rabbit secondary, was added to the sections. After more washes with TBST, SignalStain<sup>®</sup> DAB Substrate (Cell Signaling Technology, cat. 8059) was applied to sections for stain development. Sections were counterstained with hematoxylin prior to dehydration and mounting with Permount Mounting Media (Fisher Chemical, cat. SP15). Pictures were taken using a Nikon E400 microscope equipped with a Moticam 3 camera.

For immunofluorescence staining, Alexa Fluor Plus 555 secondary antibody (ThermoFisher, cat. A32732) was added for 1 hour at RT to localize DDR1, following the same protocol as described above. DDR1 was also targeted in a co-localization study to determine its presence in olfactory dendrites and neurons. To achieve this, olfactory marker protein (OMP) was targeted with a goat anti-mouse primary overnight at 4°C (gift from Dr. Frank Margolis, Professor Emeritus, University of Maryland; 1:1500) and, after washing with TBST, sections were incubated with Alexa Fluor Plus 488 (ThermoFisher, cat. A32814) for 1 hour at RT. DDR1 and OMP primary antibodies were applied to the sections simultaneously, so antibody dilutions were prepared as double the desired working concentration. The slides were washed with dH<sub>2</sub>O after the secondary incubation. For mounting and DAPI staining, Fluoromount Mounting

Medium with DAPI (ThermoFisher, cat. 00-4959-52) was used. To visualize and capture pictures of fluorescent staining, a Zeiss laser scanning confocal microscope LSM700 (Zeiss, Oberkochen, Germany), paired with Zeiss' ZEN Black software to control exposure, focus, and intensity across samples was used.

For comparison of DDR1 levels, mean fluorescent intensity (MFI) for both vehicle- (n=4) and carnosine-treated (n=4) groups was quantified using ImageJ (Shihan et al. 2021). The average MFI for each group was calculated and plotted for comparison. Standard error of the mean (SEM) of the MFI readings were used to show variance.

G Protein-Coupled Receptor 4 (GPR4):

Immunofluorescent staining was performed with sections dewaxed and hydrated as described above. Antigen retrieval was performed with SignalStain® Citrate Unmasking Solution (Cell Signaling Technology, cat. 14746), where the solution was brought to a boil and kept around 95°C for 10 minutes. The slides in solution were then cooled for 30 minutes at RT before washing with dH<sub>2</sub>O. Animal-free blocking solution was added to the slides for 1 hour at RT. Then, sections were incubated with rabbit anti-mouse GPR4 primary antibody (Novus Biologicals, cat. NLS145) at 1:90 in SignalStain® antibody diluent (Cell Signaling Technology, cat. 8812) overnight at 4°C. Co-localization studies were performed with the anti-OMP and a goat anti-mouse CYP1A1 (Daiichi Pure Chemicals, 1:250) antibodies, separately. Similar to the DDR1 co-localization protocol, antibodies were prepared at double the desired concentration, so the overnight co-incubation was performed with anti-GPR4 and CYP1A1 antibodies. After washing with TBST, Alexa Fluor Plus 488 and 555 secondary antibodies were applied to detect GPR4 and OMP/CYP1A1, respectively. The slides were washed with dH<sub>2</sub>O after the secondary

incubation. Fluoromount Mounting Medium, with DAPI (ThermoFisher, cat. 00-4959-52) was used to seal slides and provide nuclear staining. To visualize and capture pictures of fluorescent staining, we used the Zeiss laser scanning confocal microscope LSM700 (Zeiss, Oberkochen, Germany), paired with Zeiss' ZEN Black software to control exposure, focus, and intensity across samples.

Copper Metabolism MURR1 Domain Protein 1 (COMMD1):

Staining was performed with sections dewaxed and hydrated as above. Antigen retrieval was performed with SignalStain® Citrate Unmasking Solution (Cell Signaling Technology, cat. 14746), where the solution was brought to a boil and kept around 95°C for 10 minutes. The slides in solution were then cooled for 30 minutes at RT before washing with dH<sub>2</sub>O. Endogenous peroxidase was quenched with 3% hydrogen peroxide, which remained on the slides for 10 minutes at RT. Sections were washed with dH<sub>2</sub>O again. Animal-free blocking solution was added to the slides for 1 hour at RT. Then, sections were incubated with rabbit anti-mouse COMMD1 primary antibody (Proteintech cat. 11938-1-AP) at 1:250 in TBST (Cell Signaling Technology, cat. 9997) overnight at 4°C. After washing with TBST, SignalStain® Boost Detection Reagent (Cell Signaling Technology, cat. 8814), an HRP conjugated anti-rabbit secondary, was added to the sections. After more washes with TBST, SignalStain® DAB Substrate (Cell Signaling Technology, cat. 8059) was applied to sections for stain development. Sections were counterstained with hematoxylin prior to dehydration and mounting. Images were captured with the same system as above.

DnaJ Homolog C 6 (DNAJC6):

Staining was performed with sections dewaxed and hydrated the same way as above. Antigen retrieval was performed with SignalStain® Citrate Unmasking Solution (Cell Signaling Technology, cat. 14746), where the solution was brought to a boil and kept around 95°C for 10 minutes. The slides in solution were then cooled for 30 minutes at RT before washing with dH<sub>2</sub>O. Endogenous peroxidase was quenched with 3% hydrogen peroxide, which remained on the slides for 10 minutes at RT. Sections were washed with dH<sub>2</sub>O again. Animal-free blocking solution was added to the slides for 1 hour at RT. Then, sections were incubated with rabbit anti-mouse DNAJC6 primary antibody (Novus Biologicals cat. NBP1-81507) at 1:500 in SignalStain® antibody diluent (Cell Signaling Technology, cat. 8812) for 2 hours at RT before moving to 4°C overnight. After washing with TBST, SignalStain® Boost Detection Reagent (Cell Signaling Technology, cat. 8814), an HRP conjugated anti-rabbit secondary, was added to the sections. After more washes with TBST, SignalStain® DAB Substrate (Cell Signaling Technology, cat. 8059) was applied to sections for stain development. Sections were counterstained with hematoxylin prior to dehydration and mounting. Images were captured with the same system as above.

### ***Copper (II) chelation***

To evaluate carnosine's ability to chelate metals, we mixed equal parts of a 0.025M CuSO<sub>4</sub> (Sigma, cat. C-8027) working solution with carnosine (Acros Organics, New Jersey, USA) solutions of various concentrations (200 mM, 100 mM, 75 mM, 50 mM, 25 mM, 12.5 mM, 6.25 mM, 3.125 mM, 1.5625 mM, 0.78125 mM). When Cu<sup>2+</sup> interacts with a molecule's amino groups, an increasingly vibrant blue color develops; changes in this color can be measured

by UV/Vis spectrometry. Absorbance was read at 275 nm wavelength on SpectraMax M2e (Molecular Devices, San Jose, CA, USA) immediately after mixing, as described previously (Wen et al. 2017). SoftMax Pro software (Molecular Devices) processed absorbance and visualized concentration curve.

## **Results**

### ***Methylation Data Analysis of Snca and Other Genes***

RRBS was used to evaluate the methylation status of CpG islands throughout the whole mouse genome from DNA obtained from the OE. A total of 33,844 restriction fragments were aligned to the genome and identified. Only 5,734 fragments (16.9%) fell within +/- 1000 bp from the transcription start site, which shows greater potential to regulate gene expression. Out of these, 127 fragments (2.2%) showed differential methylation of 20% or greater (Table 2). Values are expressed to indicate % differences in methylation in carnosine-treated tissue compared to vehicle-treated mouse OE (Figure 2).

The initial focus was to elucidate any difference in methylation of the *Snca* regulatory CpG sites following IN carnosine treatment; however, no significant difference was observed in those regions. Other *Snca*-associated fragments showed statistically significant differences in methylation; however, they fell outside the +/- 1000 bp cutoff and did not show a differential methylation of at least 20%. Table 2 lists the differentially methylated genes and their distance from the transcription start site (TSS) and indicates genes (\*) that have a relationship to PD or other neurodegenerative diseases.

Table 2: Location and methylation status of restriction fragments and their associated genes

Gene Name	RefSeq	Distance to TSS	Differential Methylation (%)	References	
<i>Slc22a13</i>	NM_133980	-997	-28.57%	Ginsberg et al. 2011	
<i>Rab27a*</i>	NM_023635	-994	20.60%		
<i>Zfp109</i>	NM_020262	-991	-29.41%		
<i>Mir6418</i>	NR_105846	-968	31.47%		
<i>Cbarp</i>	NR_036582	-933	29.46%		
<i>Msh3</i>	NM_010829	-925	-21.86%		
<i>Ldlrad4</i>	NM_001357444	-908	-21.32%		
<i>Gm1647</i>	NR_126533	-887	29.63%		
<i>Gp1bb</i>	NM_010327	-886	22.95%		
<i>Bgn*</i>	NM_007542	-884	-32.31%		Chen et al. 2020
<i>Tgfa</i>	NM_031199	-834	21.68%		
<i>Magohb</i>	NM_025564	-829	32.24%		Boukhzar et al. 2016; Chen et al. 2019
<i>Selenow*</i>	NM_009156	-807	36.89%		
<i>Fmo9</i>	NM_001347135	-790	-25.33%		
<i>Anxa9</i>	NM_023628	-782	-22.47%	Kouchaki et al. 2018	
<i>2610035D17Rik</i>	NR_015556	-779	-23.34%		
<i>Ganab</i>	NM_001293621	-767	23.17%		
<i>Neurl1a</i>	NM_001163480	-754	20.83%		
<i>Il27ra*</i>	NM_016671	-743	-25.18%		
<i>Tysnd1</i>	NM_001272090	-738	-25.14%		
<i>Rmdn2</i>	NM_201361	-704	-38.10%		
<i>Snrnp35</i>	NM_029532	-676	30.58%		
<i>Cd81</i>	NM_133655	-622	-26.40%		
<i>Wdr34</i>	NM_001008498	-618	22.53%		
<i>Cfap20</i>	NM_008187	-603	-30.56%	Rudinskiy et al. 2009	
<i>Hpca*</i>	NM_001286081	-581	24.92%		
<i>Uap1ll</i>	NM_001033293	-579	-26.84%		
<i>Abhd5</i>	NR_152865	-574	-23.35%		
<i>Trim65</i>	NM_178802	-571	32.85%		
<i>Dgkd</i>	NM_177646	-561	-23.44%		
<i>Fbxo2l</i>	NM_145564	-550	-35.00%		
<i>Gpr4*</i>	NM_175668	-509	-26.65%		Haque et al. 2020; Haque et al. 2021
<i>Spefl</i>	NM_027641	-499	-35.00%		
<i>Ucp1*</i>	NM_009463	-480	-21.22%		Ho et al. 2012
<i>Clec10a</i>	NM_001204252	-437	-37.62%		
<i>Apobec2</i>	NM_009694	-435	-24.90%		
<i>Ppil2</i>	NM_001356386	-432	-50.00%		

<i>Dnajc6*</i>	NM_198412	-428	-25.59%	Roosen et al. 2019	
<i>Il1rn</i>	NM_031167	-410	-30.42%		
<i>Abca2</i>	NM_007379	-407	-27.65%		
<i>D130017N08Rik</i>	NR_015486	-377	-27.59%		
<i>Ankrd13c</i>	NM_001359909	-366	-21.71%		
<i>Serpnb6d</i>	NM_001076790	-362	37.14%		
<i>D16Ertd519e</i>	NR_040474	-356	23.01%		
<i>BC051019</i>	NM_001040700	-344	22.50%		
<i>Slc6a11</i>	NM_172890	-315	-20.91%		
<i>Nrsn2*</i>	NM_001009948	-314	35.46%		Nakanishi et al. 2006; Umschweif et al. 2021
<i>Gm20735</i>	NR_015497	-293	-37.50%		
<i>Tmem173</i>	NM_001289592	-292	30.36%		
<i>Tmem128</i>	NM_001356960	-251	20.84%		
<i>Lce6a</i>	NM_001166172	-226	-52.00%		
<i>5430419D17Rik</i>	NM_175166	-192	20.55%		
<i>Fbxo27</i>	NM_207238	-189	21.38%		
<i>Eid2b</i>	NM_001177427	-182	20.19%		
<i>2410004I01Rik</i>	NR_037963	-174	21.94%		
<i>Syne1</i>	NM_001347711	-127	21.86%		
<i>Mxra8</i>	NM_024263	-109	23.62%		
<i>Commd1*</i>	NM_001361661	-100	-32.04%	Vonk et al. 2014	
<i>Aatk</i>	NM_001198787	-73	-36.26%		
<i>Mir8111</i>	NR_106191	-46	22.73%		
<i>Mir7230</i>	NR_106089	-43	-22.72%		
<i>Bdh1</i>	NM_175177	16	22.75%		
<i>Olfir29-ps1</i>	NR_033638	42	21.25%		
<i>Lrrc52</i>	NM_001013382	48	-21.22%		
<i>Ffar3*</i>	NM_001033316	56	-31.75%		Hou et al. 2021
<i>Bnip3l</i>	NM_009761	79	20.68%		
<i>Olfir698</i>	NM_146602	89	-21.79%		
<i>1700066C05Rik</i>	NM_030146	105	22.25%		
<i>Olfir750</i>	NM_207558	107	24.23%		
<i>Vmn1r68</i>	NM_001172072	118	-24.19%		
<i>Hymai</i>	NR_131912	151	25.80%		
<i>Tmc4</i>	NM_181820	158	33.45%		
<i>Impact</i>	NM_001357396	184	-22.41%		
<i>Mtnr1b</i>	NM_145712	187	30.23%		
<i>Lypd4</i>	NM_182785	196	-24.23%		
<i>Gm6116</i>	NR_045866	265	32.41%		
<i>Nanos2</i>	NM_194064	271	-28.58%		
<i>Grip1osl</i>	NR_131760	284	22.76%		

<i>Fabp2</i>	NM_007980	304	25.00%	
<i>Lingo3*</i>	NM_001359746	307	-26.45%	Inoue et al. 2007; Guillemain et al. 2020
<i>D730005E14Rik</i>	NR_030675	307	20.77%	
<i>Tkfc</i>	NM_145496	322	-24.68%	
<i>Kif14</i>	NM_001287179	324	-26.22%	
<i>Lrtm1</i>	NM_176920	336	-22.44%	
<i>Ddr1*</i>	NM_172962	338	21.46%	Zhu et al. 2015; Hebron et al. 2017
<i>4930519L02Rik</i>	NM_029164	355	-58.86%	
<i>Mgarp</i>	NR_028121	358	24.27%	
<i>Nsd1</i>	NM_008739	371	20.01%	
<i>Zfp872</i>	NM_001033813	374	-20.41%	
<i>Rps19</i>	NM_001360115	385	-65.95%	
<i>Atg9b</i>	NM_001002897	388	23.98%	
<i>Col4a3</i>	NM_007734	393	-20.00%	
<i>Mir6927</i>	NR_105892	412	-22.47%	
<i>Vmn2r29</i>	NR_003555	425	-34.94%	
<i>Foxa3</i>	NM_008260	455	47.78%	
<i>Rfpl4b</i>	NM_001177783	477	21.66%	
<i>Mak</i>	NM_008547	484	-26.67%	
<i>Hand1</i>	NM_008213	521	-27.27%	
<i>Csdc2</i>	NM_145473	553	-24.24%	
<i>Mir7212</i>	NR_106071	581	24.44%	
<i>Polr2h</i>	NM_001356423	628	48.35%	
<i>Mir3569</i>	NR_106134	631	-27.04%	
<i>Gm44</i>	NM_001101450	632	-23.44%	
<i>Nat8</i>	NM_001362060	636	29.55%	
<i>Lipo3</i>	NM_001013770	664	28.00%	
<i>Tnfaip8l2</i>	NM_027206	665	-31.05%	
<i>Gm12992</i>	NR_102394	700	-26.86%	
<i>Sgcd</i>	NM_011891	704	-20.00%	
<i>Hist1h4n</i>	NM_175657	714	-26.32%	
<i>Slc38a6</i>	NM_001037717	717	-20.32%	
<i>Neat1*</i>	NR_131212	728	-31.27%	Liu & Lu 2018; Liu et al. 2020
<i>Dysf</i>	NM_001077694	740	31.00%	
<i>Hpcal4</i>	NM_174998	746	23.84%	
<i>Cisd3</i>	NM_001085500	750	-20.83%	
<i>1700012C14Rik</i>	NR_131049	759	25.67%	
<i>Ocell</i>	NM_001293800	771	23.01%	
<i>Meg3*</i>	NR_027651	798	22.04%	Quan et al. 2020

<i>Syap1</i>	NM_025932	810	27.06%	
<i>Fam71e1</i>	NM_028169	816	-29.93%	
<i>1110004E09Rik</i>	NM_026502	912	31.86%	
<i>Yif1a</i>	NM_026553	912	-22.77%	
<i>Neat1*</i>	NR_131212	925	-28.36%	Liu & Lu 2018; Liu et al. 2020
<i>Olfir90</i>	NM_146477	935	50.79%	
<i>Zfyve26</i>	NM_001008550	950	-26.97%	
<i>Dnaaf3</i>	NM_001033548	951	-34.38%	
<i>F2r*</i>	NM_010169	965	-32.52%	Zhou et al. 2011; Price et al. 2020
<i>Spc25</i>	NM_025565	985	23.61%	

**List of differentially methylated genes that were investigated for association to neurological function.** Each restriction fragment from RRBS analysis was associated with a gene name. The listed 127 fragments passed the following criteria: (1) within +/- 1000 bp of TSS of the respective gene and (2) differential methylation of +/- 20%. \*Genes associated with PD or neurological function

After a literature search of the 127 gene fragments that met criteria, several genes had previous research showing an association to PD, including discoidin domain receptor 1 (*Ddr1*), G protein-coupled receptor 4 (*Gpr4*), DnaJ homolog C 6 (*Dnajc6*), and copper metabolism MURR1 domain protein 1 (*Commd1*). From our RRBS analysis, DNA methylation was increased by 21.5% in a potentially regulatory region of the *Ddr1* gene after IN carnosine treatment, signifying a decrease in mRNA and protein level downstream (Table 2). For *Gpr4*, the carnosine treated mice had 26.65% less methylation on its potentially regulatory fragment, signifying an increase in transcript expression and protein level. That trend continued for both *Dnajc6* and *Commd1*, which had 25.59% and 32.04% less methylation, respectively.

The methylation profile for each fragment varied between treatment and is able to be visualized with IGV (Figure 3). Increased methylation after carnosine treatment for the *Ddr1*-associated fragment is represented by an increase in the amount of red on the chart when compared to the vehicle group (Figure 3A). Conversely, hypomethylation is shown for *Gpr4*,

*Dnajc6*, and *Commd1* by a decrease in red after carnosine treatment (Figure 3B-D). Analyzing transcript expression and protein localization to the OE via RT-qPCR and immunostaining, respectively, will provide us with further information on how differential methylation of these fragments affects them downstream.

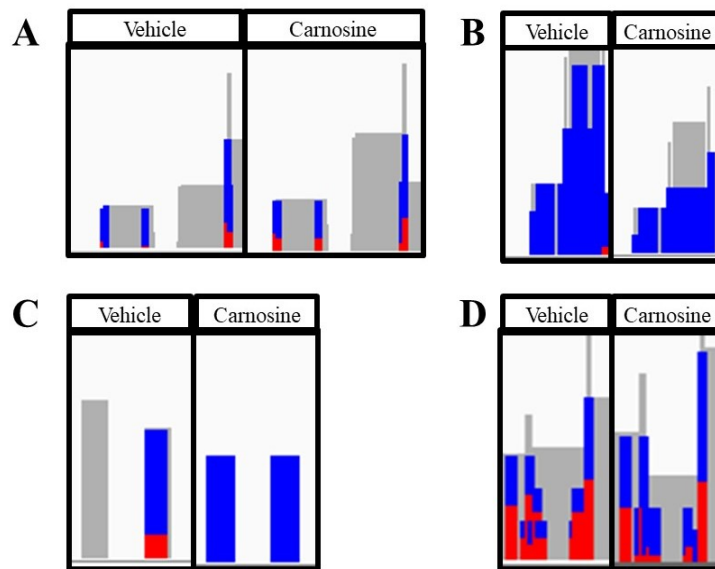


**Figure 3. Alignment of *Ddr1*, *Gpr4*, *Dnajc6*, and *Commd1* fragments displays differential methylation profile exhibited by carnosine treatment.** The BAM files produced from RRBS analysis contain genome sequence and methylation information. Files were uploaded into Integrative Genomics Viewer (IGV) for sequence alignment and visualization of methylation differences. These diagrams located the *Ddr1* (A), *Gpr4* (B), *Dnajc6* (C), and *Commd1* (D) fragments. The red regions are areas of hypermethylation. In combination with the quantitative data for these fragments, *Ddr1* shows hypermethylation, while *Gpr4*, *Dnajc6*, and *Commd1* show hypomethylation after carnosine treatment.

## RT-qPCR

To evaluate the downstream effects of the methylation changes discussed above, RT-qPCR was performed with RNA isolated from mouse OE tissue. *Snca*, *Ddr1*, and *Gpr4* Ct values were evaluated for vehicle treated (n=2) and IN carnosine treated (n=2) samples, and relative expression was calculated with *Actb* and the  $2^{-\Delta\Delta C_t}$  method (sample size was limited due to RNA degradation in other stored samples). In mice treated with IN carnosine, there was no difference in *Snca* expression, which corresponds to the lack of methylation change observed in the RRBS analysis (Figure 4A). *Ddr1* and *Gpr4* both showed near-2-fold decreases after IN carnosine treatment (Figure 4B-C). The *Ddr1* result corresponds with the increased methylation reported from the RRBS analysis. However, *Gpr4* expression would have been expected to increase based on its decreased methylation.

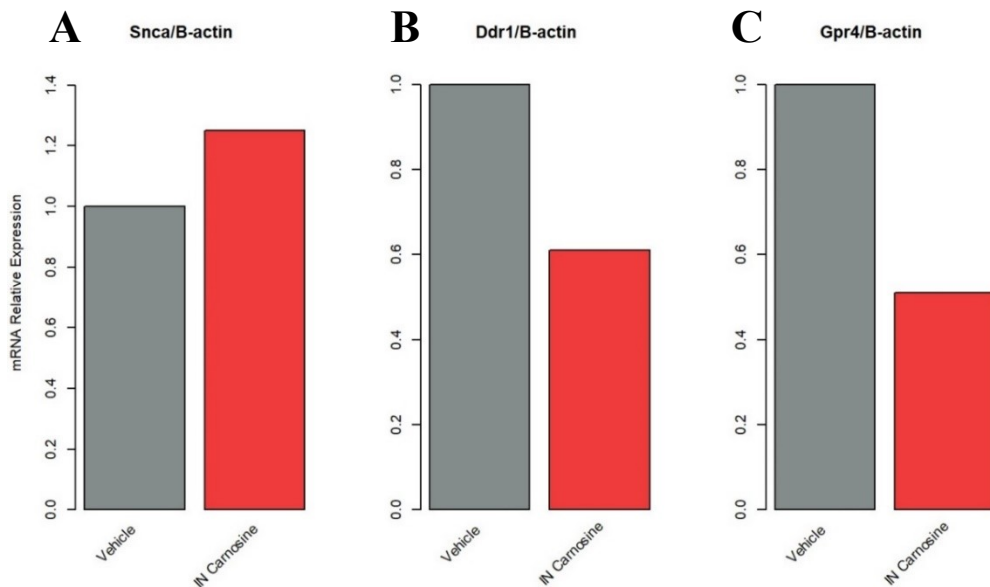


**Figure 4. Gene expression analysis of *Snca*, *Ddr1*, and *Gpr4* in mice treated with carnosine.** RT-qPCR analysis was performed with olfactory epithelial tissue to verify observed methylation changes from RRBS analysis for *Snca* (A), *Ddr1* (B), and *Gpr4* (C). Vehicle treated mice (n=2) were administered dH<sub>2</sub>O, while IN Carnosine treated mice (n=2) were given 2 mg/day. Expression of each gene was calculated relative to *β-actin*.

## *Immunostaining*

DDR1:

When considering how the other genes of interest may affect aSyn levels in the OE, a first step was to elucidate the cellular localization of these proteins. To observe DDR1 in mouse OE, we used anti-DDR1 antibody and developed the stain with DAB as the chromogen (Figure 5). This experiment showed that DDR1 is present in the OE and nerve bundles of the nasal cavity in vehicle and carnosine treated mice (Figure 5A-B). At higher magnification, staining was observed in the dendrites of olfactory neurons in the OE (Figure 5C).

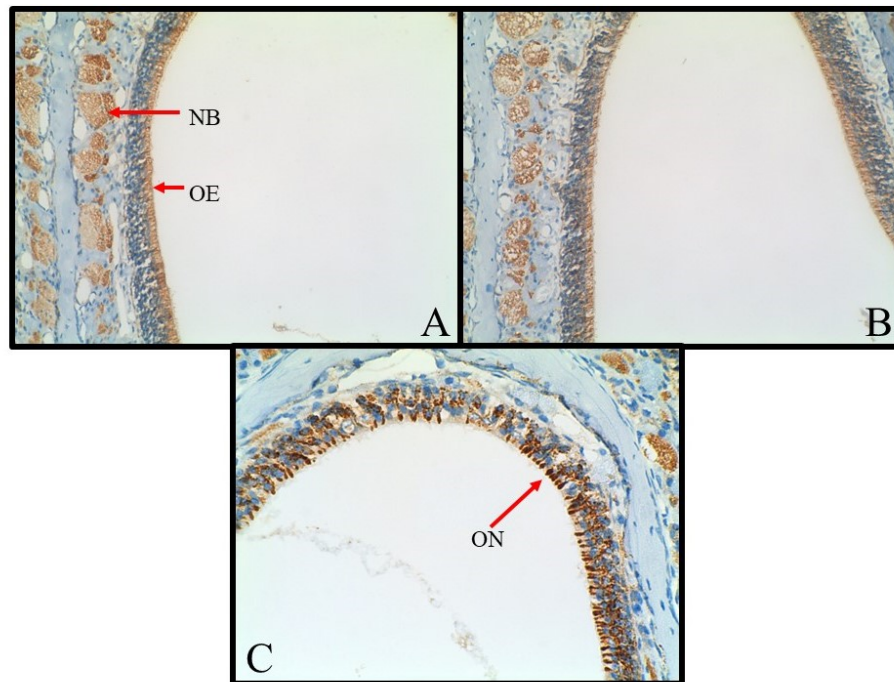


**Figure 5. Immunohistochemistry staining suggests DDR1 localization to olfactory neurons and nerve bundles in the olfactory mucosa.** DAB development showed DDR1 in the olfactory epithelium and nerve bundles of vehicle (A) and carnosine treated (B) mice (20X). Dendrites of olfactory neurons with DDR1 present are seen at higher magnification (40X) (C). Sections were counterstained with hematoxylin. OE: Olfactory epithelium; NB: Nerve bundle; ON: Olfactory neuron.

To confirm localization of DDR1 to olfactory neurons, a co-localization experiment was performed with olfactory marker protein (OMP), which is known to localize to mature neurons of the OE (Johnson et al. 1993) (Figure 6). The yellow fluorescence represents overlap between DDR1 and OMP, which can be in olfactory nerve cell bodies and projections toward the surface of the epithelium. Fluorescent signal from the nerve bundles further supports the presence of DDR1 in neurons throughout olfactory neurons (Figure 6D-E). Signal development settings were kept constant during image acquisition to ensure reliable fluorescence quantification.

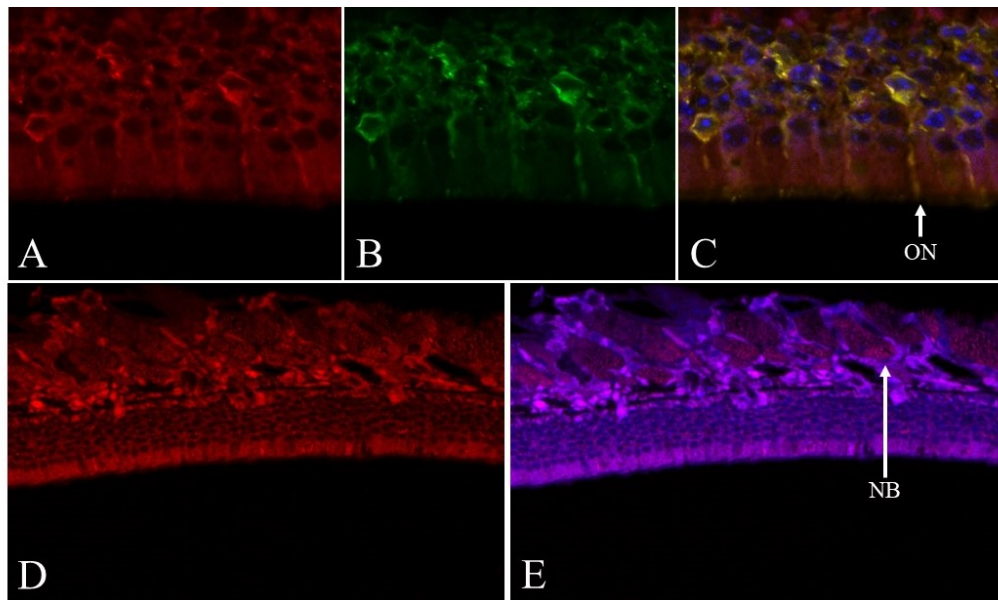


**Figure 6. Immunofluorescent co-localization with OMP confirms the presence of DDR1 in olfactory neurons and nerve bundles.** DDR1 (A) is present throughout the olfactory epithelium (20X). OMP (B) is present in the epithelium and appears to fluoresce more intensely in the olfactory neurons (20X). DDR1 and OMP co-localization confirmed the presence of DDR1 in dendrites of olfactory neurons (C) (20X). Further study confirmed DDR1 is present in the nerve bundles, signifying its localization to neurons throughout the olfactory epithelium (red signal D-E). ON: Olfactory neuron; NB: Nerve bundle.

To further elucidate potential effects of methylation differences on downstream DDR1 levels, we used ImageJ to quantify the difference in mean fluorescence intensity (MFI) between vehicle (n=4) and carnosine treated groups (n=4) (Shihan et al. 2021). No significant difference in MFI was observed between the two treatment groups (-12.2%,  $p=0.40$ ) (Figure 7). Based on the differential methylation and mRNA expression results for *Ddr1*, the difference in protein level quantified using MFI would have been expected to decrease in mice treated with carnosine.

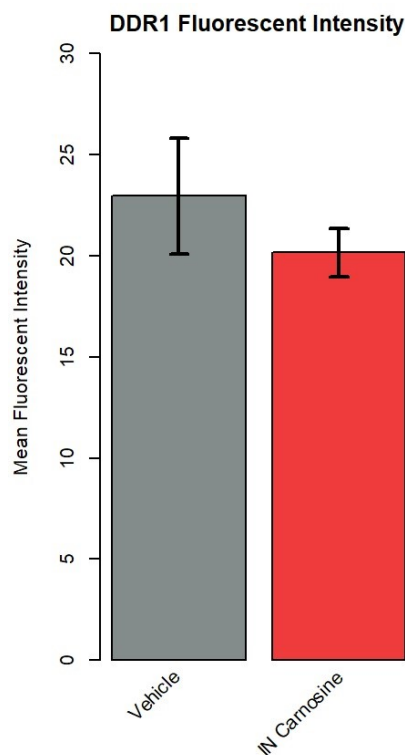


**Figure 7. DDR1 protein level did not change in carnosine-treated mice.**

Immunofluorescence staining was used to quantify the amount of DDR1 in the OE. Mean fluorescent intensity (MFI) was calculated with ImageJ. Vehicle-treated mice OE sections (n=4) had 12.2% more DDR1 than carnosine-treated mice (n=4), but this was not statistically significant ( $p=0.40$ ). Error bars represent standard error of the mean (SEM).

## GPR4:

Since the homogenized olfactory mucosa tissue, containing multiple cell types, was utilized for RRBS analysis, immunolocalization of GPR4 in the OE was evaluated for future understanding of its potential function. Similar to DDR1, we compared GPR4 immunolocalization to that of OMP to evaluate GPR4's potential presence in olfactory neurons (Figure 8). The neurons fluoresced with the green signal of OMP, but GPR4 was not present in the same cells (8 B-C). However, the GPR4 signal (red) appears to localize in Bowman's glands and the ducts of Bowman's glands leading to the surface of the epithelium (8 A-C). To further confirm localization to Bowman's glands and ducts, co-localization of GPR4 and CYP1A1 was used to identify whether those regions with GPR4 fluorescence are Bowman's glands or olfactory ducts. CYP1A1 and other cytochrome P450 enzymes have been immunolocalized to Bowman's glands, with some predicted to be secreted by Bowman's glands (Voight et al. 1993; Genter et al. 2006). This was an unexpected finding, as an additional role of GPR4 is in pain perception, so immunolocalization to trigeminal nerve fibers in the epithelium was the expected outcome (Ru et al. 2015; Miltz et al. 2017; Velcicky et al. 2017).

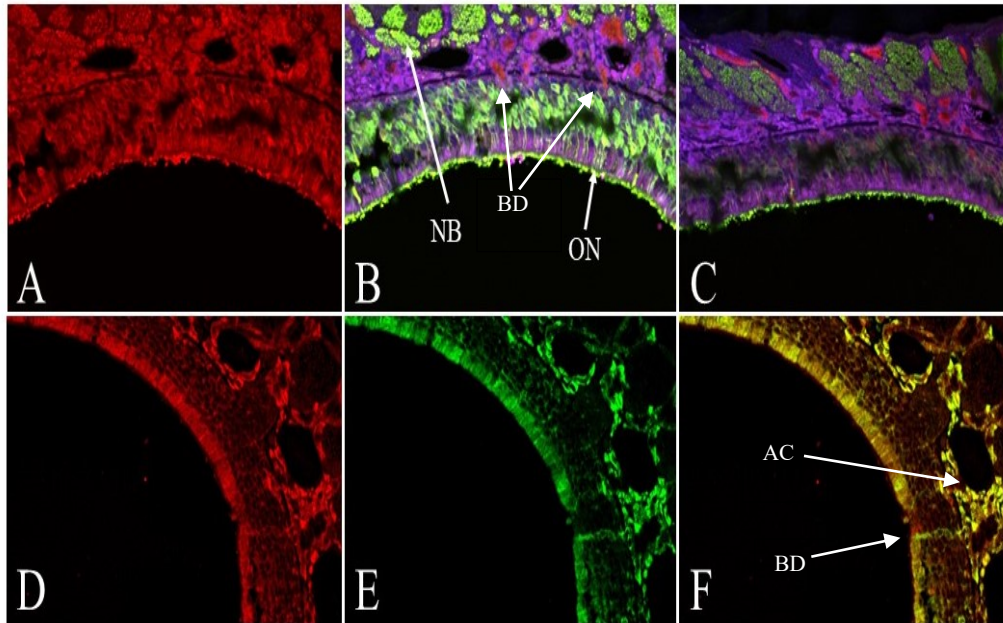


**Figure 8. Immunofluorescent co-localization shows absence of GPR4 in neurons and presence in the ducts of Bowman's glands in the mouse olfactory epithelium.** GPR4 (A) is present throughout the olfactory epithelium (20X). OMP (B) is present in the epithelium, but it appears the fluorescence is more intense in the olfactory neurons (ON) and subepithelial nerve bundles (NB) (20X). GPR4 and OMP co-localization showed a lack of GPR4 in olfactory neurons; however, GPR4 appears to localize to the acinar cells of Bowman's glands (AC) and within ducts of Bowman's glands (C) (20X). Further study confirmed GPR4 is present in the ducts of Bowman's glands via co-localization with CYP1A1 (D-E). ON: Olfactory neuron; NB: Nerve bundle; AC: Acinar cells; BD: Duct of Bowman's gland.

## DNAJC6:

Previous studies have identified selective expression of DNAJC6 in neurons, so we would expect to find that DNAJC6 localizes to olfactory neurons and nerve bundles in the olfactory mucosa (Edvardson et al. 2012). The immunostaining pattern shows signal development along the apical surface of the epithelium, which could potentially signify the presence of DNAJC6 in the dendrites of olfactory neurons (Figure 9). Also, staining appears in the nerve bundles that are found below the basal membrane and near the top of the field of view (Figure 9).

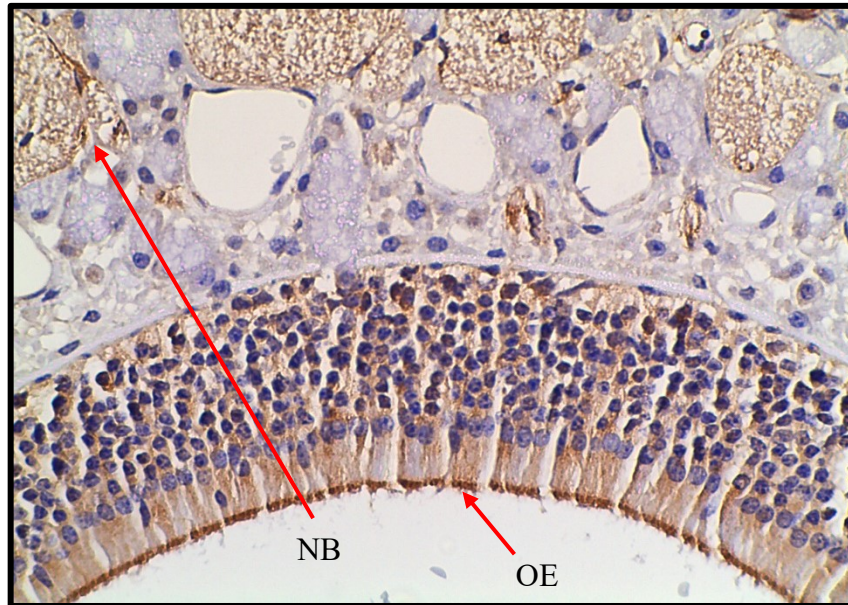


**Figure 9. Immunohistochemistry staining shows the presence of DNAJC6 in the nerve bundles and along the surface of the olfactory epithelium.** DAB development showed DNAJC6 near the apical surface of the epithelium (OE), which may include the dendrites of olfactory neurons, and nerve bundles (NB) of the olfactory epithelium in mice (40X). Sections were counterstained with hematoxylin.

COMMD1:

To localize COMMD1 in mouse OE, we used anti-COMMD1 antibody and developed the stain with DAB as the chromogen (Figure 10). This experiment showed that COMMD1 is present in the sustentacular cells and Bowman's glands of the OE (Figure 10).

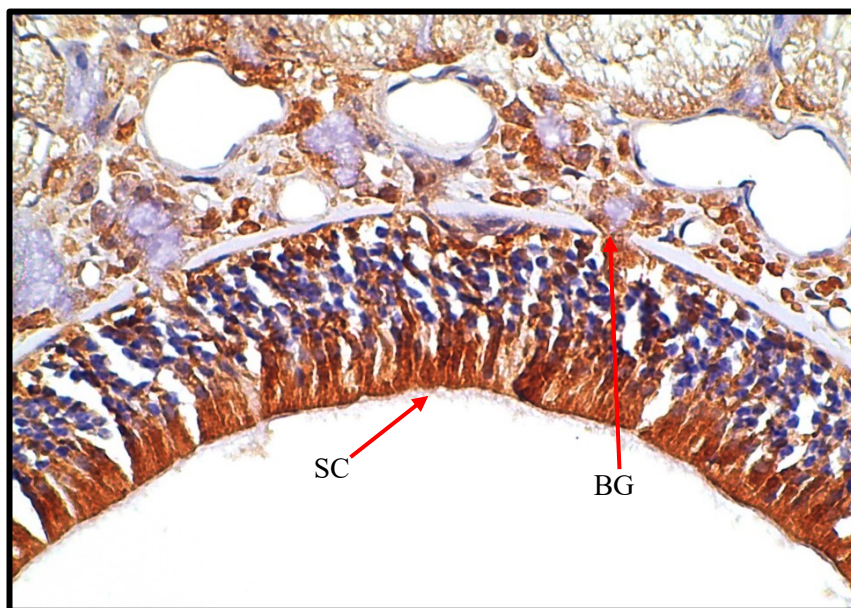


**Figure 10. Immunohistochemistry staining shows the presence of COMMD1 in the sustentacular cells and ducts of Bowman's glands in the olfactory mucosa. DAB development showed COMMD1 in the sustentacular cells (SC) and the ducts of Bowman's glands (BG) of the olfactory epithelium in mice (40X). Sections were counterstained with hematoxylin.**

### ***Copper (Cu<sup>2+</sup>) Chelation***

Due to the difference in methylation of *Commd1* in our RRBS analysis, its role in copper homeostasis, and previous reports of carnosine's metal-chelating activity, we investigated the potential ability of carnosine to chelate Cu<sup>2+</sup> (Gromadzka et al. 2020; Boldyrev et al. 2013). The method used was based on previous observations that showed the amine groups of polyethyleneimine form a complex with copper, which produces a blue color that shows maximum absorption at a wavelength of 275 nm (Wen et al. 2017). As shown in Figure 1,

carnosine has 4 amine groups available to interact with  $\text{Cu}^{2+}$  ions. In our investigation, copper sulfate ( $\text{CuSO}_4$ ) was briefly incubated with varying concentrations of carnosine to establish the minimum carnosine concentration required to maximize absorbance at 275 nm. The absorbance maximum occurs with carnosine concentrations greater than 12.5 mM or a ratio of 0.5 moles of carnosine per mole of  $\text{Cu}^{2+}$  (Figure 11).

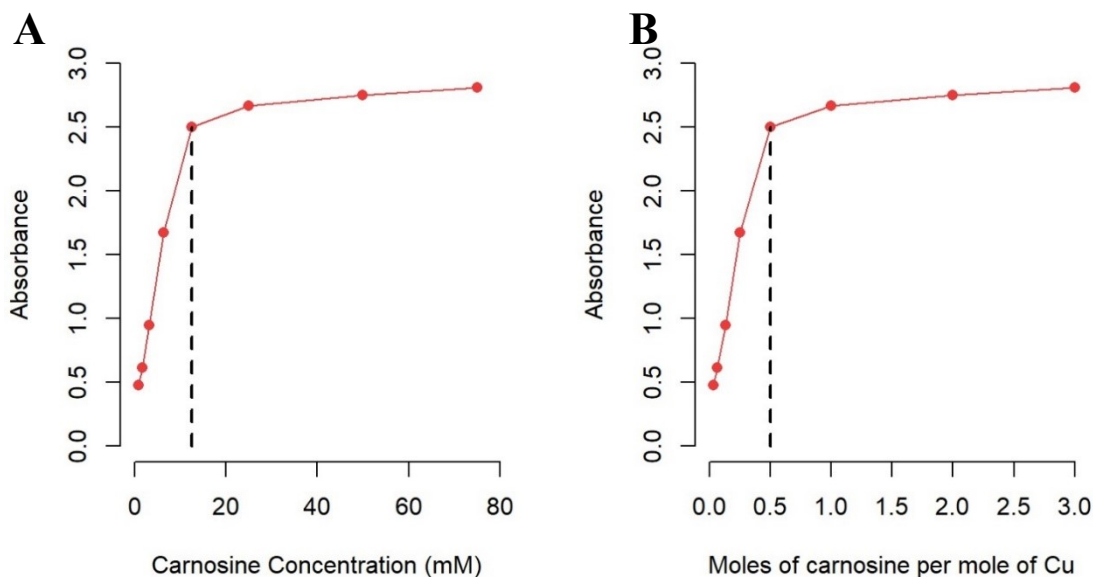


**Figure 11. Assessment of carnosine- $\text{Cu}^{2+}$  complex formation using absorbance confirms carnosine's ability to chelate copper.** Absorbance measured at 275 nm determined that 12.5 mM carnosine was the concentration where maximum chelation of  $\text{Cu}^{2+}$  occurs (A). For every mole of  $\text{Cu}^{2+}$ , 0.5 moles of carnosine are required to achieve maximum complex formation (B).

### ***Pathway Analysis***

ToppFun was used for functional enrichment analysis to identify pathways that may be affected by IN carnosine treatment. Every fragment within 1000 bp of the TSS was split into one of two groups: increased or decreased methylation after carnosine treatment. Subsequently, the list of genes from each group was processed in ToppFun, which provided Gene Ontology (GO) pathways significantly associated with the change in that group. Pathway analysis showed the relationship between IN carnosine treatment and epigenetic changes of neurological pathways

(Figure 12). Hypomethylated pathways, such as neurotransmitter transport and synaptic signaling, would be expected to have genes with increased expression, potentially improving activity of those pathways. Conversely, genes in hypermethylated pathways would be predicted to have decreased expression and lower activity. Affected genes were determined to be involved with regulation of neurogenesis and nervous system development. There are also three shared pathways between the two groups: brain development, neuron projection, and neuron projection morphogenesis.

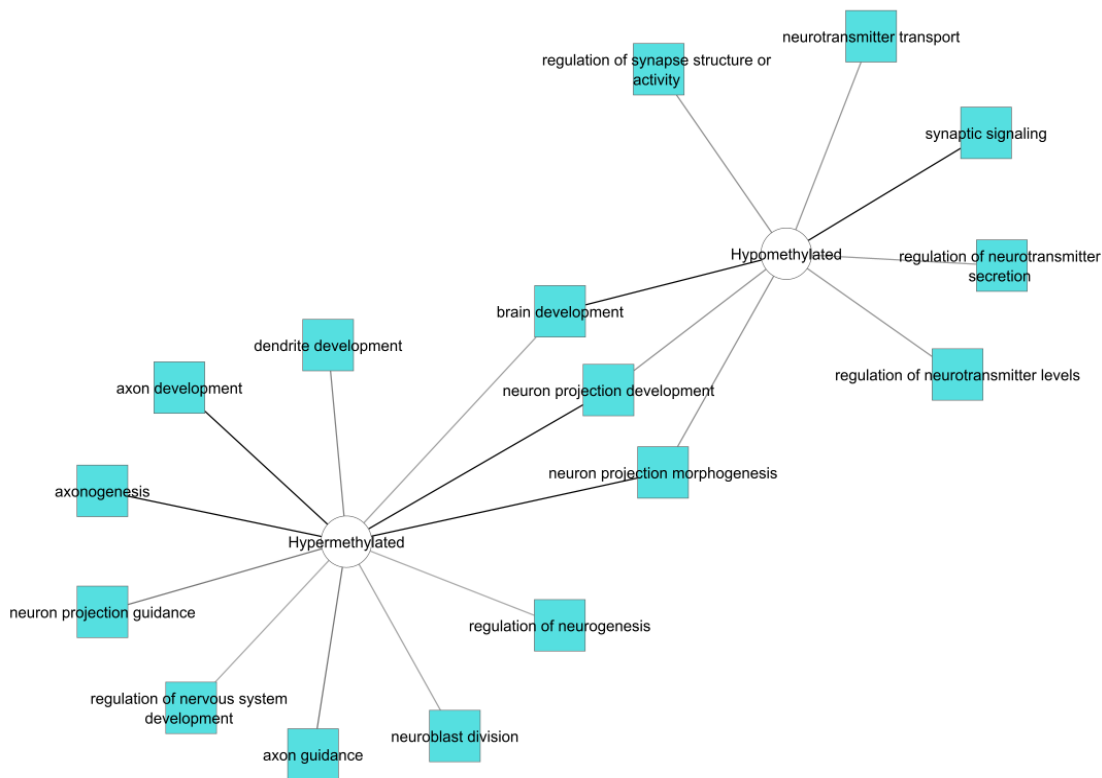


**Figure 12. Pathway analysis network map displays trend of neurological pathways affected by differential methylation in carnosine-treated mice.** Based on Gene Ontology output from ToppFun, an interaction network was constructed using Cytoscape. The hypermethylated group refers to gene fragments that had increased methylation after carnosine treatment. The hypomethylated group refers to gene fragments that had decreased methylation after carnosine treatment.

## **Discussion**

### ***RRBS and Methylation of PD-related Genes***

Global DNA methylation analysis, as we have performed, has not been previously conducted in the context of PD or carnosine. Studies have used similar methods to analyze pathways affected by methylation in other neurological diseases, such as Huntington's disease and Alzheimer's disease (Ng et al. 2012; Altuna et al. 2019). Our gene-specific approach evaluated criteria, such as distance to the TSS and proportional methylation, to identify genes that could have altered downstream expression as a result of differential methylation between vehicle and carnosine treated mice. Initially, our study evaluated *Snca*, which is widely implicated in development and progression of PD through overexpression or aggregation of aSyn (Spillatini et al. 1998; Brás and Outeiro 2021). Based on previous findings, IN carnosine treatment in mice was shown to decrease aSyn aggregation in the OE (Bermúdez et al. 2019). Our RRBS analysis showed that regulatory CpG islands associated with *Snca* were not significantly methylated, signifying that decreased aSyn accumulation is not due to differential methylation.

Following *Snca*, a literature review was performed on each gene associated to a fragment that passed our evaluation criteria to see if there has been an established connection to PD or another neurological disease. From that list, four genes were identified for further analysis: *Ddr1*, *Gpr4*, *Dnajc6*, and *Commd1*. In our analysis, increased methylation of a *Ddr1* promoter was observed, which corresponds with decreased *Ddr1* expression. DDR1 is a tyrosine kinase that plays a role in cell proliferation and differentiation. It is present throughout the CNS and has been shown to have increased expression in the brains of post-mortem PD patients (Zhu et al. 2015; Hebron et al. 2017). Clearance of neurotoxic proteins, such as aSyn, was increased in mice

treated with nilotinib, an inhibitor of DDR1 activity (Hebron et al. 2013). Knockdown of DDR1 levels was also associated with increased clearance of aSyn in mice (Hebron et al. 2017). These previous results identified DDR1 as a putative drug target for PD. A decrease in DDR1 levels after carnosine treatment corresponds with the previously observed aSyn decrease resulting from inhibited/knocked-out DDR1 *in vivo*. If carnosine affects downstream production of DDR1, that provides reasoning for the decreased amount of aSyn in the OE of mice treated with carnosine (Bermúdez et al. 2019).

GPR4 is a receptor that is present in vascular endothelial cells and in neurons throughout the brain, where it plays a role in pro-inflammatory responses and respiration, respectively (Krewson et al. 2020; Hosford et al. 2018). It has been associated with promotion of inflammation and cancer cell progression (Wang et al. 2018; Yu et al. 2019). In the context of PD, GPR4 inhibition/knockout has been shown to decrease the pro-apoptotic effects of MPP<sup>+</sup> treatment *in vitro* (Haque et al. 2020). Further, *in vivo* inhibition of GPR4 protected mice treated with MPTP from neuronal loss in the SN, the brain region most associated with PD (Haque et al. 2021). The SN is the brain region most affected in PD patients, and carnosine treatment in patients has been shown to improve clinical outcomes (Boldyrev et al. 2008). Therefore, the neuroprotective effect of GPR4 may be realized with increased methylation and, therefore, decreased expression downstream. However, our RRBS analysis showed decreased methylation in carnosine-treated mice, contradicting the perceived beneficial effect of GPR4.

The DNAJC protein family plays an important role in vesicular transport with clathrin-coated vesicles (CCVs) and protection against misfolded/denatured proteins via stimulation of heat shock proteins (HSPs) (Umeda et al. 2000; Stetler et al. 2010). Auxilin, encoded by *Dnajc6*, is primarily responsible for uncoating CCVs and is selectively expressed in neurons (Edvardson

et al. 2012). *Dnajc6* mutations, which affect auxilin function in neurons, have been associated with juvenile parkinsonism and early-onset PD (Köroğlu et al. 2013; Olgiati et al. 2016; Roosen et al. 2019). Although a mechanism has not been elucidated, endocytosis of clathrin-coated synaptic vesicles is impaired by auxilin loss of function (Morgan et al. 2001). CCVs are present in olfactory receptor neurons, where they play a crucial role in endocytosis of odorant receptors, so we would expect to find auxilin present in olfactory neurons in the epithelium (Mashukova et al. 2006). After carnosine treatment, a fragment associated with *Dnajc6* showed decreased methylation, potentially increasing expression. If decreased function of auxilin favors development of PD, then increased expression resulting from carnosine treatment could be beneficial in protecting against PD by improving synaptic transmission and decreasing misfolded protein.

COMMD1 is a protein that specifically binds to  $\text{Cu}^{2+}$  and interacts with other proteins, such as NF- $\kappa$ B, to alter their activity or increase ubiquitination and subsequent proteolysis (Narindrasorasak et al. 2007; Maine et al. 2007). COMMD1 protein-protein interactions play a role in copper homeostasis and copper transport diseases. Menkes disease results from a mutation in *ATP7A*, a copper transporter, which can be bound by COMMD1, restoring its copper export function (Vonk et al. 2012). In neurodegenerative disorders, such as Alzheimer's disease and PD, copper dysregulation has been implicated in various pathologies, including protein aggregation (Gromadzka et al. 2020). While COMMD1 has not been directly associated with a role in copper toxicity in the brain, it has been shown to improve clearance of aggregated Parkin, a protein that is implicated in PD progression, so it may also be involved in clearance of aSyn as well (Vonk et al. 2014). Further, an interaction between copper, COMMD1, and protein aggregates in the brain could provide a basis for COMMD1 activity in PD. If COMMD1 levels

increase after treatment, an additive metal-chelating effect could be achieved due to the individual chelating activities of carnosine and COMMD1 (Narindrasorasak et al. 2007, Boldyrev et al. 2013). Between improved protein degradation and copper regulation, increased levels of COMMD1 show potential for preventing PD or delaying the progression of the disease.

### ***mRNA Expression***

After identifying genes of interest from the RRBS analysis, we investigated downstream effects to evaluate how the epigenetic differences between treatment groups could affect potential pathologies, starting with RT-qPCR. Using the primers listed in Table 1, we evaluated mRNA expression of *Snca*, *Ddr1*, and *Gpr4*, which were normalized to  $\beta$ -actin. The relative expression of each gene was shown and compared to the respective methylation profile; however, the sample size was not large enough to evaluate statistical significance.

Differential methylation of the *Snca* promoter was not observed with RRBS, and the mRNA expression corresponded to that, showing no difference between treatment groups. *Ddr1* and *Gpr4* portrayed significant differential methylation of regulatory regions in the RRBS analysis, but both genes showed near-two-fold changes in expression after carnosine treatment. *Ddr1* expression decreased, which corresponds to the observed increased methylation in carnosine-treated mice. However, the expression difference for *Gpr4* did not correspond to its methylation profile; transcript expression decreased when it would have been expected to increase based on the decreased methylation in the one CpG site. If there is a more crucial regulatory CpG site that was unchanged after carnosine treatment, that could explain why differential methylation on the evaluated fragment may not lead to the difference predicted by the methylation profile.

## ***Immunostaining***

When evaluating methylation or transcript expression in homogenized mouse OE tissue, it is impossible to understand where the protein that corresponds to the target gene localizes *in vivo*. Elucidating cell-specific expression could be crucial in hypothesizing potential mechanism of action or role of a protein, which promotes future research. In the context of this study, DDR1, GPR4, DNAJC6, and COMMD1 have all been associated with neurological function, but their location in the mouse OE had yet to be identified (Hebron et al. 2013; Haque et al. 2021; Roosen et al. 2019; Vonk et al. 2014).

DDR1 has been shown to be expressed in the CNS, specifically in neurons (Zhu et al. 2015). In Figures 5 and 6, we show that DDR1 localizes to the nerve bundles and the dendrites of olfactory neurons throughout the OE. By co-staining with olfactory marker protein (OMP), which is specifically found in mature olfactory receptor neurons, we were able to demonstrate the presence of DDR1 in the olfactory neurons (Farbman & Margolis 1980). With its presence in neurons in the OE and brain, DDR1 could play a role in the observed of decreased aSyn aggregation in the OE and SN in carnosine-treated mice (Bermúdez et al. 2019, Brown et al. 2021). Intranasally-administered carnosine has been shown to penetrate to the olfactory bulb via the axons of olfactory neurons, showing its potential to reach deeper brain regions (Burd et al. 1982). So, carnosine treatment could potentiate the action of DDR1 in decreasing aSyn in the midbrain and improving clinical symptoms, as reported (Brown et al. 2021; Boldyrev et al. 2008). Further, we utilized immunofluorescence to quantify a treatment-specific effect on DDR1 levels in the OE, which showed no significant difference between the treatment groups (Figure 7).

Previously, GPR4 has been localized to vascular endothelial cells and neurons in various brain regions, but it has not been identified in mouse OE (Huang et al. 2007; Hosford et al. 2018). Similarly to DDR1, we attempted to co-localize GPR4 with OMP to identify its presence in olfactory neurons, but no overlap was present. However, GPR4 fluorescence appeared in the acinar cells and ducts of Bowman's glands, which has not been previously shown. To confirm this, co-localization was performed with CYP1A1, an enzyme previously predicted to be present in and secreted by Bowman's glands in the olfactory mucosa (Voight et al. 1993; Genter et al. 2006).

DNAJC6 has previously been reported to be expressed in neurons, but this had not yet been clarified in the olfactory mucosa (Edvardson et al. 2012). Our studies show DNAJC6 localizes near the apical surface of the OE and in nerve bundles. This signifies that DNAJC6 might be specifically expressed in the dendrites of olfactory receptor neurons. In the cell, DNAJC6 is responsible for removing clathrin from CCVs, so its presence near the interface of the epithelium and the nasal cavity could infer a role in internalization of olfactory receptors that must undergo endocytosis (Mashukova et al. 2006). Moreover, clathrin is one of the proteins that helps form synaptic vesicles responsible for neurotransmission, so improving functionality of endocytosis could prove beneficial in mitigating the characteristic motor deficits observed in PD (Kononenko et al. 2014).

COMMD1 is a ubiquitously expressed protein that has been reported to play a crucial role in hepatic copper regulation and protein ubiquitination (Burstein et al. 2005; Maine et al. 2007; Vonk et al. 2011). In the olfactory mucosa, COMMD1 appears to be expressed in the sustentacular cells and Bowman's glands, but further co-localization studies need to be performed to confirm this observation. The presence of COMMD1 in the OE portrays its

potential to be involved in decreasing aSyn aggregation observed after carnosine treatment (Bermúdez et al. 2019). Similar to DDR1, COMMD1 is expressed in the brain, so carnosine localization to deeper brain regions could promote increased COMMD1 activity, decreasing aSyn in the SN and improving clinical outcomes (Boldyrev et al. 2008; Brown et al. 2021).

### ***Carnosine Chelation of Copper (II)***

Dysregulation of copper homeostasis has been implicated in several neurological diseases, including PD (Gromadzka et al 2020). Knowing COMMD1's role in copper regulation and carnosine's metal-chelating properties, we investigated whether carnosine is able to efficiently chelate  $\text{Cu}^{2+}$  through an absorbance-based assay (Vonk et al. 2014). Using various concentrations of carnosine, we generated a concentration curve which showed that a 12.5 mM carnosine solution is sufficient to maximize absorbance at 275nm wavelength, signifying that only 0.5 moles of carnosine are required to chelate the  $\text{Cu}^{2+}$  available in solution. The carnosine- $\text{Cu}^{2+}$  complex forms due to interactions between amine groups in carnosine (Figure 1) and  $\text{Cu}^{2+}$ ; the reactivity between amine groups and  $\text{Cu}^{2+}$  was previously established with polyethyleneimine (PEI), which required 4 moles of PEI for each mole of  $\text{Cu}^{2+}$  (Wen et al. 2017). Based on the association of copper dysregulation and PD, carnosine's ability to chelate  $\text{Cu}^{2+}$  and potentially increase COMMD1 activity provides reason for the observed decrease in aSyn aggregation in mice and improved clinical outcomes in PD patients (Boldyrev et al. 2008; Bermúdez et al. 2019, Brown et al. 2021).

### ***Pathway Analysis***

One commonly utilized method to analyze global methylation data is functional enrichment, which can determine pathways whose genes are most commonly affected by a

treatment, such as carnosine in this study. We used ToppFun to perform our analysis and found a trend of affected pathways related to the nervous system and neurogenesis (Chen et al. 2009). The RRBS data was split into two groups: increased methylation and decreased methylation in carnosine-treated mice. This style of analysis does not provide insight into how the function of each pathway may be affected. For example, genes related to synaptic signaling tend to be hypomethylated after carnosine treatment, which means their expression would be expected to increase. However, the genes involved in synaptic signaling could be beneficial or detrimental to the pathway, so it can be difficult to discern whether carnosine is improving or worsening each pathway.

Interestingly, *DDR1*, *aSyn*, and *DNAJC6* have each been associated with several of the affected pathways. *DDR1* is associated with cell proliferation, which could play a role in developmental pathways, such as brain and neuron projection development (Zhu et al. 2015). These are mostly associated with hypermethylation in our analysis, just as the *Ddr1* fragment was hypermethylated in the carnosine-treated mice in the RRBS analysis. Conversely, the hypomethylated cluster includes pathways related to signaling, including neurotransmitter transport and synaptic signaling. This also relates to our genes of interest, *Snca* and *Dnajc6*, which encode proteins involved with the function of vesicles in signaling (Maroteaux et al. 1988; Umeda et al. 2000). *DNAJC6* assists in uncoating CCVs, which are found in olfactory receptor neurons in the OE, and *aSyn* commonly localizes to presynaptic terminals (Mashukova et al. 2006).

### **Future Directions**

To further this line of research and elucidate more of the beneficial mechanism of IN carnosine, more studies can be performed to investigate other genes and proteins. There are other

genes that we were unable to study that we believe warrant further consideration as genes of interest. These genes still passed all quantitative criteria from the RRBS analysis, such as distance to TSS and methylation difference, but lacked the strong associations to neurologic function or ability to measure downstream effects with RT-qPCR and immunostaining. One example is ribosomal protein S 19 (*Rps19*). *Rps19* is one of the constituent proteins of the small 40S subunit of ribosomes (Caterino et al. 2014). In our RRBS analysis, the *Rps19*-associated fragment was 65.95% less methylated in carnosine-treated mice. This was the largest absolute difference out of the 127 fragments that passed the evaluation criteria. However, there is a lack of literature on how its function may affect aSyn aggregation or PD phenotypes, despite the potentially large change in expression resulting from the differential methylation.

Two other genes that warrant future investigation are uncoupling protein 1 (*Ucp1*) and Nuclear Paraspeckle Assembly Transcript 1 (*Neat1*). *Ucp1* encodes UCP1, which is a mitochondrial protein that endogenously reduces the production of ROS resulting from oxidative phosphorylation (Ho et al 2012). In our analysis, *Ucp1* was hypomethylated in carnosine-treated mice (-21.22%). Mitochondrial function and oxidative stress are thought to promote development and progression of PD, so a protein that alleviates that risk, such as UCP1, could be beneficial (Winklhofer and Haass 2010; Dias et al. 2013). NEAT1 is a long non-coding RNA that has been associated with PD (Liu & Lu 2018; Liu et al. 2020). In the RRBS results, there were two fragments associated with *Neat1*, and they both portrayed substantial changes (-31.27% and -28.36%). Further research could likely be done with both genes to further the scope of the methylation data.

To develop the findings on genes we have already analyzed, there are two steps we can take: increase sample size for gene expression analysis and continue with immunostaining for

DNAJC6 and COMMD1. Using immunofluorescent analysis, similar to what was utilized for DDR1 and GPR4, we could confirm localization of DNAJC6 and COMMD1 to olfactory neurons and Bowman's glands, respectively. Further, we can assess how carnosine treatment affects protein levels, which could then be compared to the RRBS data to evaluate how differential methylation affects downstream expression. When isolating RNA for reverse transcription and subsequent qPCR analysis, we lacked a substantial number of viable samples to develop the desired statistical power. In future studies, harvesting OE tissue from more mice would provide us with enough data to find potentially significant changes in transcript expression. As for DNAJC6 and COMMD1 immunostaining, we have been unable to identify a reliable protocol for localizing the proteins. With more resources, localizing the protein in the OE and quantifying the difference in protein level between treatment groups could provide reason to continue research into the relationship between carnosine and DNAJC6. Similarly, quantifying the difference in COMMD1 protein level via immunofluorescent staining could provide insight into how hypomethylation of the *Commd1* fragment in carnosine-treated mice corresponds to downstream effects on protein and activity.

## **Conclusions**

Epigenetic changes are considered a mechanism for regulation of downstream protein expression and may be an effective target in the development of therapeutics. The present study shows that IN carnosine treatment affects methylation patterns of regulatory DNA regions of genes whose proteins are associated with neurological function and disease, such as *Ddr1*, *Gpr4*, *Dnajc6*, and *Commd1*. Further, carnosine treatment promoted methylation changes in several pathways related to neurogenesis, brain development, and synaptic signaling. Being able to synthesize gene-specific and global genome analyses could be crucial to understanding how

carnosine treatment induces observed reduction in aSyn and marked improvement in motor deficits in mice and humans that are attributed to PD (Boldyrev et al. 2008; Bermúdez et al. 2019; Brown et al. 2021). However, the reduction in aSyn aggregation in the OE of mice that has been previously shown after carnosine treatment did not correspond to differential methylation of the potential regulatory CpG sites we examined that are associated with *Snca*. Future studies should continue to investigate the mechanism by which IN carnosine treatment reduces aSyn in the OE.

Determining the localization of the proteins encoded by our genes of interest via immunostaining in the OE may also further the understanding of mechanism by which carnosine leads to reduction of aSyn. Each protein may play its own role in the cellular biology that leads to the development and progression of PD, and interpreting differences in a protein's activity in various tissues, such as the OE and SN, could prove vital to progressing therapeutic interventions in the future.

## **Bibliography**

- Ahlskog JE, Muentner MD. 2001. Frequency of levodopa-related dyskinesias and motor fluctuations as estimated from the cumulative literature: Levodopa Motor Complication Frequency. *Mov Disord.* 16(3):448–458. <http://dx.doi.org/10.1002/mds.1090>.
- Alonso Cánovas A, Luquin Piudo R, García Ruiz-Espiga P, Burguera JA, Campos Arillo V, Castro A, Linazasoro G, López Del Val J, Vela L, Martínez Castrillo JC. 2014. Agonistas dopaminérgicos en la enfermedad de Parkinson. *Neurología.* 29(4):230–241. <http://dx.doi.org/10.1016/j.nrl.2011.04.012>.
- Altuna M, Urdániz-Casado A, Sánchez-Ruiz de Gordo J, Zelaya MV, Labarga A, Lepesant JM, Roldán M, Blanco-Luquin I, Perdonés Á, Larumbe R, et al. 2019. DNA methylation signature of human hippocampus in Alzheimer’s disease is linked to neurogenesis. *Clin Epigenetics.* 11(1):91. <http://dx.doi.org/10.1186/s13148-019-0672-7>.
- Bae O-N, Serfozo K, Baek S-H, Lee KY, Dorrance A, Rumble W, Fitzgerald SD, Farooq MU, Naravelta B, Bhatt A, et al. 2013. Safety and efficacy evaluation of carnosine, an endogenous neuroprotective agent for ischemic stroke. *Stroke.* 44(1):205–212. <http://dx.doi.org/10.1161/STROKEAHA.112.673954>.
- Bartels T, Kim NC, Luth ES, Selkoe DJ. 2014. N-alpha-acetylation of  $\alpha$ -synuclein increases its helical folding propensity, GM1 binding specificity and resistance to aggregation. *PLoS One.* 9(7):e103727. <http://dx.doi.org/10.1371/journal.pone.0103727>.
- Bellia F, Vecchio G, Rizzarelli E. 2014. Carnosinases, their substrates and diseases. *Molecules.* 19(2):2299–2329. <http://dx.doi.org/10.3390/molecules19022299>.
- Bermúdez M-L, Seroogy KB, Genter MB. 2019. Evaluation of carnosine intervention in the Thy1-aSyn mouse model of Parkinson’s disease. *Neuroscience.* 411:270–278. <http://dx.doi.org/10.1016/j.neuroscience.2019.05.026>.
- Bermúdez M-L, Skelton MR, Genter MB. 2018. Intranasal carnosine attenuates transcriptomic alterations and improves mitochondrial function in the Thy1-aSyn mouse model of Parkinson’s disease. *Mol Genet Metab.* 125(3):305–313. <http://dx.doi.org/10.1016/j.ymgme.2018.08.002>.
- Bhidayasiri R, Garcia Ruiz PJ, Henriksen T. 2016. Practical management of adverse events related to apomorphine therapy. *Parkinsonism Relat Disord.* 33:S42–S48. <http://dx.doi.org/10.1016/j.parkreldis.2016.11.017>.
- Blake LE, Roux J, Hernando-Herraez I, Banovich NE, Perez RG, Hsiao CJ, Eres I, Cuevas C, Marques-Bonet T, Gilad Y. 2020. A comparison of gene expression and DNA methylation patterns across tissues and species. *Genome Res.* 30(2):250–262. <http://dx.doi.org/10.1101/gr.254904.119>.
- Bolam JP, Brown MTC, Moss J, Magill PJ. 2009. Basal ganglia: Internal organization. In: *Encyclopedia of Neuroscience.* Elsevier. p. 97–104.

- Boldyrev A, Fedorova T, Stepanova M, Dobrotvorskaya I, Kozlova E, Boldanova N, Bagyeva G, Ivanova-Smolenskaya I, Illarioshkin S. 2008. Carnosine increases efficiency of DOPA therapy of Parkinson's disease: a pilot study. *Rejuvenation Res.* 11(4):821–827. <http://dx.doi.org/10.1089/rej.2008.0716>.
- Boldyrev AA, Aldini G, Derave W. 2013. Physiology and pathophysiology of carnosine. *Physiol Rev.* 93(4):1803–1845. <http://dx.doi.org/10.1152/physrev.00039.2012>.
- Borghain R, Szasz J, Stanzione P, Meshram C, Bhatt M, Chirilineau D, Stocchi F, Lucini V, Giuliani R, Forrest E, et al. 2014. Randomized trial of safinamide add-on to levodopa in Parkinson's disease with motor fluctuations: Safinamide Add-On to L-Dopa in Mid-to-Late PD. *Mov Disord.* 29(2):229–237. <http://dx.doi.org/10.1002/mds.25751>.
- Boukhar L, Hamieh A, Cartier D, Tanguy Y, Alsharif I, Castex M, Arabo A, El Hajji S, Bonnet J-J, Errami M, et al. 2016. Selenoprotein T exerts an essential oxidoreductase activity that protects dopaminergic neurons in mouse models of Parkinson's disease. *Antioxid Redox Signal.* 24(11):557–574. <http://dx.doi.org/10.1089/ars.2015.6478>.
- Brás IC, Outeiro TF. 2021. Alpha-synuclein: Mechanisms of release and pathology progression in synucleinopathies. *Cells.* 10(2):375. <http://dx.doi.org/10.3390/cells10020375>.
- Brown JM, Baker LS, Seroogy KB, Genter MB. 2021. Intranasal carnosine mitigates  $\alpha$ -synuclein pathology and motor dysfunction in the Thy1-aSyn mouse model of Parkinson's disease. *ACS Chem Neurosci.* 12(13):2347–2359. <http://dx.doi.org/10.1021/acscchemneuro.1c00096>.
- Burd GD, Davis BJ, Macrides F, Grillo M, Margolis FL. 1982. Carnosine in primary afferents of the olfactory system: an autoradiographic and biochemical study. *J Neurosci.* 2(2):244–255. <http://dx.doi.org/10.1523/jneurosci.02-02-00244.1982>.
- Burstein E, Hoberg JE, Wilkinson AS, Rumble JM, Csomos RA, Komarck CM, Maine GN, Wilkinson JC, Mayo MW, Duckett CS. 2005. COMMD proteins, a novel family of structural and functional homologs of MURR1. *J Biol Chem.* 280(23):22222–22232. <http://dx.doi.org/10.1074/jbc.M501928200>.
- Caterino M, Aspesi A, Pavesi E, Imperlini E, Pagnozzi D, Ingenito L, Santoro C, Dianzani I, Ruoppolo M. 2014. Analysis of the interactome of ribosomal protein S19 mutants. *Proteomics.* 14(20):2286–2296. <http://dx.doi.org/10.1002/pmic.201300513>.
- Chen J, Bardes EE, Aronow BJ, Jegga AG. 2009. ToppGene Suite for gene list enrichment analysis and candidate gene prioritization. *Nucleic Acids Res.* 37(Web Server issue):W305–11. <http://dx.doi.org/10.1093/nar/gkp427>.
- Chen L, Periquet M, Wang X, Negro A, McLean PJ, Hyman BT, Feany MB. 2009. Tyrosine and serine phosphorylation of alpha-synuclein have opposing effects on neurotoxicity and soluble oligomer formation. *J Clin Invest.* 119(11):3257–3265. <http://dx.doi.org/10.1172/JCI39088>.
- Chen P, Wang C, Liu Qing, Tian J, Liu Qiong. 2019. Identification of FAM96B as a novel selenoprotein W binding partner in the brain. *Biochem Biophys Res Commun.* 512(1):137–143. <http://dx.doi.org/10.1016/j.bbrc.2019.02.139>.

- Chen S, Guo D, Lei B, Bi J, Yang H. 2020. Biglycan protects human neuroblastoma cells from nitric oxide-induced death by inhibiting AMPK-mTOR mediated autophagy and intracellular ROS level. *Biotechnol Lett.* 42(4):657–668. <http://dx.doi.org/10.1007/s10529-020-02818-z>.
- Chen SW, Drakulic S, Deas E, Ouberai M, Aprile FA, Arranz R, Ness S, Roodveldt C, Guilliams T, De-Genst EJ, et al. 2015. Structural characterization of toxic oligomers that are kinetically trapped during  $\alpha$ -synuclein fibril formation. *Proc Natl Acad Sci U S A.* 112(16):E1994-2003. <http://dx.doi.org/10.1073/pnas.1421204112>.
- Choi SY, Kwon HY, Kwon OB, Kang JH. 1999. Hydrogen peroxide-mediated Cu,Zn-superoxide dismutase fragmentation: protection by carnosine, homocarnosine and anserine. *Biochim Biophys Acta Gen Subj.* 1472(3):651–657. [http://dx.doi.org/10.1016/s0304-4165\(99\)00189-0](http://dx.doi.org/10.1016/s0304-4165(99)00189-0).
- Damier P, Hirsch EC, Agid Y, Graybiel AM. 1999. The substantia nigra of the human brain. *Brain.* 122(8):1437–1448. <http://dx.doi.org/10.1093/brain/122.8.1437>.
- Deleu D, Hanssens Y, Northway MG. 2004. Subcutaneous apomorphine: An evidence-based review of its use in Parkinson's disease. *Drugs Aging.* 21(11):687–709. <http://dx.doi.org/10.2165/00002512-200421110-00001>.
- Dias V, Junn E, Mouradian MM. 2013. The role of oxidative stress in Parkinson's disease. *J Parkinsons Dis.* 3(4):461–491. <http://dx.doi.org/10.3233/JPD-130230>.
- Edvardson S, Cinnamon Y, Ta-Shma A, Shaag A, Yim Y-I, Zenvirt S, Jalas C, Lesage S, Brice A, Taraboulos A, et al. 2012. A deleterious mutation in DNAJC6 encoding the neuronal-specific clathrin-uncoating co-chaperone auxilin, is associated with juvenile parkinsonism. *PLoS One.* 7(5):e36458. <http://dx.doi.org/10.1371/journal.pone.0036458>.
- Ellis CE, Schwartzberg PL, Grider TL, Fink DW, Nussbaum RL. 2001. A-synuclein is phosphorylated by members of the src family of protein-tyrosine kinases. *J Biol Chem.* 276(6):3879–3884. <http://dx.doi.org/10.1074/jbc.m010316200>.
- Ellis JM, Fell MJ. 2017. Current approaches to the treatment of Parkinson's Disease. *Bioorg Med Chem Lett.* 27(18):4247–4255. <http://dx.doi.org/10.1016/j.bmcl.2017.07.075>.
- Eryilmaz IE, Cecener G, Erer S, Egeli U, Tunca B, Zarifoglu M, Elibol B, Bora Tokcaer A, Saka E, Demirkiran M, et al. 2017. Epigenetic approach to early-onset Parkinson's disease: low methylation status of SNCA and PARK2 promoter regions. *Neurol Res.* 39(11):965–972. <http://dx.doi.org/10.1080/01616412.2017.1368141>.
- Farbman AI, Margolis FL. 1980. Olfactory marker protein during ontogeny: immunohistochemical localization. *Dev Biol.* 74(1):205–215. [http://dx.doi.org/10.1016/0012-1606\(80\)90062-7](http://dx.doi.org/10.1016/0012-1606(80)90062-7).
- Fearnley JM, Lees AJ. 1991. AGEING AND PARKINSON'S DISEASE: SUBSTANTIA NIGRA REGIONAL SELECTIVITY. *Brain.* 114(5):2283–2301. <http://dx.doi.org/10.1093/brain/114.5.2283>.

- Fowler AJ, Hebron M, Balaraman K, Shi W, Missner AA, Greenzaid JD, Chiu TL, Ullman C, Weatherdon E, Duka V, et al. 2020. Discoidin Domain Receptor 1 is a therapeutic target for neurodegenerative diseases. *Hum Mol Genet.* 29(17):2882–2898. <http://dx.doi.org/10.1093/hmg/ddaa177>.
- Fujiwara H, Hasegawa M, Dohmae N, Kawashima A, Masliah E, Goldberg MS, Shen J, Takio K, Iwatsubo T. 2002. alpha-Synuclein is phosphorylated in synucleinopathy lesions. *Nat Cell Biol.* 4(2):160–164. <http://dx.doi.org/10.1038/ncb748>.
- Gasser T. 2009. Molecular pathogenesis of Parkinson disease: insights from genetic studies. *Expert Rev Mol Med.* 11(e22):e22. <http://dx.doi.org/10.1017/S1462399409001148>.
- Genter MB, Van Veldhoven PP, Jegga AG, Sakthivel B, Kong S, Stanley K, Witte DP, Ebert CL, Aronow BJ. 2003. Microarray-based discovery of highly expressed olfactory mucosal genes: potential roles in the various functions of the olfactory system. *Physiol Genomics.* 16(1):67–81. <http://dx.doi.org/10.1152/physiolgenomics.00117.2003>.
- Genter MB, Yost GS, Rettie AE. 2006. Localization of CYP4B1 in the rat nasal cavity and analysis of CYPs as secreted proteins. *J Biochem Mol Toxicol.* 20(3):139–141. <http://dx.doi.org/10.1002/jbt.20123>.
- Ginsberg SD, Mufson EJ, Alldred MJ, Counts SE, Wu J, Nixon RA, Che S. 2011. Upregulation of select rab GTPases in cholinergic basal forebrain neurons in mild cognitive impairment and Alzheimer's disease. *J Chem Neuroanat.* 42(2):102–110. <http://dx.doi.org/10.1016/j.jchemneu.2011.05.012>.
- Grivennikova VG, Maklashina EO, Gavrikova EV, Vinogradov AD. 1997. Interaction of the mitochondrial NADH-ubiquinone reductase with rotenone as related to the enzyme active/inactive transition. *Biochim Biophys Acta Bioenerg.* 1319(2–3):223–232. [http://dx.doi.org/10.1016/s0005-2728\(96\)00163-6](http://dx.doi.org/10.1016/s0005-2728(96)00163-6).
- Gromadzka G, Tarnacka B, Flaga A, Adamczyk A. 2020. Copper dyshomeostasis in neurodegenerative diseases-therapeutic implications. *Int J Mol Sci.* 21(23):9259. <http://dx.doi.org/10.3390/ijms21239259>.
- Grosset KA, Malek N, Morgan F, Grosset DG. 2013. Inhaled apomorphine in patients with “on-off” fluctuations: a randomized, double-blind, placebo-controlled, clinic and home based, parallel-group study. *J Parkinsons Dis.* 3(1):31–37. <http://dx.doi.org/10.3233/JPD-120142>.
- Guillemain A, Laouarem Y, Cobret L, Štefok D, Chen W, Bloch S, Zahaf A, Blot L, Reverchon F, Normand T, et al. 2020. LINGO family receptors are differentially expressed in the mouse brain and form native multimeric complexes. *FASEB J.* 34(10):13641–13653. <http://dx.doi.org/10.1096/fj.202000826R>.
- Haque ME, Akther M, Azam S, Choi D-K, Kim I-S. 2020. GPR4 knockout improves the neurotoxin-induced, caspase-dependent mitochondrial apoptosis of the dopaminergic neuronal cell. *Int J Mol Sci.* 21(20):7517. <http://dx.doi.org/10.3390/ijms21207517>.

- Haque ME, Azam S, Akther M, Cho D-Y, Kim I-S, Choi D-K. 2021. The neuroprotective effects of GPR4 inhibition through the attenuation of caspase mediated apoptotic cell death in an MPTP induced mouse model of Parkinson's disease. *Int J Mol Sci.* 22(9). <http://dx.doi.org/10.3390/ijms22094674>.
- Hartman PE, Hartman Z, Ault KT. 1990. Scavenging of singlet molecular oxygen by imidazole compounds: high and sustained activities of carboxy terminal histidine dipeptides and exceptional activity of imidazole-4-acetic acid. *Photochem Photobiol.* 51(1):59–66. <http://dx.doi.org/10.1111/j.1751-1097.1990.tb01684.x>.
- Hebron M, Peyton M, Liu X, Gao X, Wang R, Lonskaya I, Moussa CE-H. 2017. Discoidin domain receptor inhibition reduces neuropathology and attenuates inflammation in neurodegeneration models. *J Neuroimmunol.* 311:1–9. <http://dx.doi.org/10.1016/j.jneuroim.2017.07.009>.
- Hebron ML, Lonskaya I, Moussa CE-H. 2013. Nilotinib reverses loss of dopamine neurons and improves motor behavior via autophagic degradation of  $\alpha$ -synuclein in Parkinson's disease models. *Hum Mol Genet.* 22(16):3315–3328. <http://dx.doi.org/10.1093/hmg/ddt192>.
- Heinz S, Benner C, Spann N, Bertolino E, Lin YC, Laslo P, Cheng JX, Murre C, Singh H, Glass CK. 2010. Simple combinations of lineage-determining transcription factors prime cis-regulatory elements required for macrophage and B cell identities. *Mol Cell.* 38(4):576–589. <http://dx.doi.org/10.1016/j.molcel.2010.05.004>.
- Ho PW, Ho JW, Liu H-F, So DH, Tse ZH, Chan K-H, Ramsden DB, Ho S-L. 2012. Mitochondrial neuronal uncoupling proteins: a target for potential disease-modification in Parkinson's disease. *Transl Neurodegener.* 1(1):3. <http://dx.doi.org/10.1186/2047-9158-1-3>.
- Hodge GK, Butcher LL. 1980. Pars compacta of the substantia nigra modulates motor activity but is not involved importantly in regulating food and water intake. *Naunyn Schmiedebergs Arch Pharmacol.* 313(1):51–67. <http://dx.doi.org/10.1007/bf00505805>.
- Horisaka K, Nakayama S, Okazaki M, Miyashita Y, Sakaki H, Miyasaka M, Morimoto Y. 1974. PHARMACOLOGICAL STUDIES OF L-CARNOSINE (N-2-M) 1st REPORT: General pharmacological activities. *Journal of The Showa Medical Association.* 34(3):271–283. <http://dx.doi.org/10.14930/jsma1939.34.271>.
- Hosford PS, Mosienko V, Kishi K, Jurisic G, Seuwen K, Kinzel B, Ludwig MG, Wells JA, Christie IN, Koolen L, et al. 2018. CNS distribution, signalling properties and central effects of G-protein coupled receptor 4. *Neuropharmacology.* 138:381–392. <http://dx.doi.org/10.1016/j.neuropharm.2018.06.007>.
- Hou Y-F, Shan C, Zhuang S-Y, Zhuang Q-Q, Ghosh A, Zhu K-C, Kong X-K, Wang S-M, Gong Y-L, Yang Y-Y, et al. 2021. Gut microbiota-derived propionate mediates the neuroprotective effect of osteocalcin in a mouse model of Parkinson's disease. *Microbiome.* 9(1):34. <http://dx.doi.org/10.1186/s40168-020-00988-6>.
- Huang F, Mehta D, Predescu S, Kim KS, Lum H. 2007. A novel lysophospholipid- and pH-sensitive receptor, GPR4, in brain endothelial cells regulates monocyte transmigration. *Endothelium.* 14(1):25–34. <http://dx.doi.org/10.1080/10623320601177288>.

- Inglis KJ, Chereau D, Brigham EF, Chiou S-S, Schöbel S, Frigon NL, Yu M, Caccavello RJ, Nelson S, Motter R, et al. 2009. Polo-like kinase 2 (PLK2) phosphorylates alpha-synuclein at serine 129 in central nervous system. *J Biol Chem.* 284(5):2598–2602. <http://dx.doi.org/10.1074/jbc.C800206200>.
- Inoue H, Lin L, Lee X, Shao Z, Mendes S, Snodgrass-Belt P, Sweigard H, Engber T, Pepinsky B, Yang L, et al. 2007. Inhibition of the leucine-rich repeat protein LINGO-1 enhances survival, structure, and function of dopaminergic neurons in Parkinson's disease models. *Proc Natl Acad Sci U S A.* 104(36):14430–14435. <http://dx.doi.org/10.1073/pnas.0700901104>.
- Islam MS, Azim F, Saju H, Zargarani A, Shirzad M, Kamal M, Fatema K, Rehman S, Azad MAM, Ebrahimi-Barough S. 2021. Pesticides and Parkinson's disease: Current and future perspective. *J Chem Neuroanat.* 115(101966):101966. <http://dx.doi.org/10.1016/j.jchemneu.2021.101966>.
- Jadhav K, Gambhire M, Shaikh I, Kadam V, Pisal S. 2007. Nasal drug delivery system-factors affecting and applications. *Curr Drug ther.* 2(1):27–38. <http://dx.doi.org/10.2174/157488507779422374>.
- Johnson EW, Eller PM, Jafek BW. 1993. An immuno-electron microscopic comparison of olfactory marker protein localization in the supranuclear regions of the rat olfactory epithelium and vomeronasal organ neuroepithelium. *Acta Otolaryngol.* 113(6):766–771. <http://dx.doi.org/10.3109/00016489309135898>.
- Kalia LV, Lang AE. 2015. Parkinson's disease. *Lancet.* 386(9996):896–912. [http://dx.doi.org/10.1016/s0140-6736\(14\)61393-3](http://dx.doi.org/10.1016/s0140-6736(14)61393-3).
- Kalinderi K, Bostantjopoulou S, Fidani L. 2016. The genetic background of Parkinson's disease: current progress and future prospects. *Acta Neurol Scand.* 134(5):314–326. <http://dx.doi.org/10.1111/ane.12563>.
- Kamal MA, Keep RF, Smith DE. 2008. Role and relevance of PEPT2 in drug disposition, dynamics, and toxicity. *Drug Metab Pharmacokinet.* 23(4):236–242. <http://dx.doi.org/10.2133/dmpk.23.236>.
- Khoo TK, Yarnall AJ, Duncan GW, Coleman S, O'Brien JT, Brooks DJ, Barker RA, Burn DJ. 2013. The spectrum of nonmotor symptoms in early Parkinson disease. *Neurology.* 80(3):276–281. <http://dx.doi.org/10.1212/WNL.0b013e31827deb74>.
- Kish SJ, Perry TL, Hansen S. 1979. Regional distribution of homocarnosine, homocarnosine-synthetase and homocarnosinase in human brain. *J Neurochem.* 32(6):1629–1636. <http://dx.doi.org/10.1111/j.1471-4159.1979.tb02272.x>.
- Kononenko NL, Puchkov D, Classen GA, Walter AM, Pechstein A, Sawade L, Kaempf N, Trimbuch T, Lorenz D, Rosenmund C, et al. 2014. Clathrin/AP-2 mediate synaptic vesicle reformation from endosome-like vacuoles but are not essential for membrane retrieval at central synapses. *Neuron.* 82(5):981–988. <http://dx.doi.org/10.1016/j.neuron.2014.05.007>.

- Kopin IJ. 1987. MPTP: an industrial chemical and contaminant of illicit narcotics stimulates a new era in research on Parkinson's disease. *Environ Health Perspect.* 75:45–51. <http://dx.doi.org/10.1289/ehp.877545>.
- Köroğlu Ç, Baysal L, Cetinkaya M, Karasoy H, Tolun A. 2013. DNAJC6 is responsible for juvenile parkinsonism with phenotypic variability. *Parkinsonism Relat Disord.* 19(3):320–324. <http://dx.doi.org/10.1016/j.parkreldis.2012.11.006>.
- Kouchaki E, Kakhaki RD, Tamtaji OR, Dadgostar E, Behnam M, Nikouejad H, Akbari H. 2018. Increased serum levels of TNF- $\alpha$  and decreased serum levels of IL-27 in patients with Parkinson disease and their correlation with disease severity. *Clin Neurol Neurosurg.* 166:76–79. <http://dx.doi.org/10.1016/j.clineuro.2018.01.022>.
- Krewson EA, Sanderlin EJ, Marie MA, Akhtar SN, Velcicky J, Loetscher P, Yang LV. 2020. The proton-sensing GPR4 receptor regulates paracellular gap formation and permeability of vascular endothelial cells. *iScience.* 23(2):100848. <http://dx.doi.org/10.1016/j.isci.2020.100848>.
- Langston JW, Ballard P, Tetrud JW, Irwin I. 1983. Chronic Parkinsonism in humans due to a product of meperidine-analog synthesis. *Science.* 219(4587):979–980. <http://dx.doi.org/10.1126/science.6823561>.
- Langston JW, Forno LS, Rebert CS, Irwin I. 1984. Selective nigral toxicity after systemic administration of 1-methyl-4-phenyl-1,2,5,6-tetrahydropyridine (MPTP) in the squirrel monkey. *Brain Res.* 292(2):390–394. [http://dx.doi.org/10.1016/0006-8993\(84\)90777-7](http://dx.doi.org/10.1016/0006-8993(84)90777-7).
- Langston JW, Irwin I, Langston EB, Forno LS. 1984. 1-Methyl-4-phenylpyridinium ion (MPP<sup>+</sup>): identification of a metabolite of MPTP, a toxin selective to the substantia nigra. *Neurosci Lett.* 48(1):87–92. [http://dx.doi.org/10.1016/0304-3940\(84\)90293-3](http://dx.doi.org/10.1016/0304-3940(84)90293-3).
- de Lau LML, Breteler MMB. 2006. Epidemiology of Parkinson's disease. *Lancet Neurol.* 5(6):525–535. [http://dx.doi.org/10.1016/S1474-4422\(06\)70471-9](http://dx.doi.org/10.1016/S1474-4422(06)70471-9).
- Lauren K. Wolf. 2013. The pesticide connection. *Chem Eng News Archive.* 91(47):11–15. <http://dx.doi.org/10.1021/cen-09147-cover>.
- Lesage S, Brice A. 2009. Parkinson's disease: from monogenic forms to genetic susceptibility factors. *Hum Mol Genet.* 18(R1):R48-59. <http://dx.doi.org/10.1093/hmg/ddp012>.
- Licker V, Côte M, Lobrinus JA, Rodrigo N, Kövari E, Hochstrasser DF, Turck N, Sanchez J-C, Burkhard PR. 2012. Proteomic profiling of the substantia nigra demonstrates CNDP2 overexpression in Parkinson's disease. *J Proteomics.* 75(15):4656–4667. <http://dx.doi.org/10.1016/j.jprot.2012.02.032>.
- Liu J, Liu D, Zhao B, Jia C, Lv Y, Liao J, Li K. 2020. Long non-coding RNA NEAT1 mediates MPTP/MPP<sup>+</sup>-induced apoptosis via regulating the miR-124/KLF4 axis in Parkinson's disease. *Open Life Sci.* 15(1):665–676. <http://dx.doi.org/10.1515/biol-2020-0069>.
- Liu Y, Lu Z. 2018. Long non-coding RNA NEAT1 mediates the toxic of Parkinson's disease induced by MPTP/MPP<sup>+</sup> via regulation of gene expression. *Clin Exp Pharmacol Physiol.* 45(8):841–848. <http://dx.doi.org/10.1111/1440-1681.12932>.

- Lücking CB, Dürr A, Bonifati V, Vaughan J, De Michele G, Gasser T, Harhangi BS, Meco G, Denèfle P, Wood NW, et al. 2000. Association between early-onset Parkinson's disease and mutations in the parkin gene. *N Engl J Med.* 342(21):1560–1567.  
<http://dx.doi.org/10.1056/NEJM200005253422103>.
- Maine GN, Mao X, Komarck CM, Burstein E. 2007. COMMD1 promotes the ubiquitination of NF-kappaB subunits through a cullin-containing ubiquitin ligase. *EMBO J.* 26(2):436–447.  
<http://dx.doi.org/10.1038/sj.emboj.7601489>.
- Margolis FL. 1974. Carnosine in the primary olfactory pathway. *Science.* 184(4139):909–911.  
<http://dx.doi.org/10.1126/science.184.4139.909>.
- Maroteaux L, Campanelli JT, Scheller RH. 1988. Synuclein: a neuron-specific protein localized to the nucleus and presynaptic nerve terminal. *J Neurosci.* 8(8):2804–2815. 1988.  
<http://dx.doi.org/10.1523/jneurosci.08-08-02804.1988>.
- Mashukova A, Spehr M, Hatt H, Neuhaus EM. 2006. Beta-arrestin2-mediated internalization of mammalian odorant receptors. *J Neurosci.* 26(39):9902–9912.  
<http://dx.doi.org/10.1523/JNEUROSCI.2897-06.2006>.
- Matsumoto L, Takuma H, Tamaoka A, Kurisaki H, Date H, Tsuji S, Iwata A. 2010. CpG demethylation enhances alpha-synuclein expression and affects the pathogenesis of Parkinson's disease. *PLoS One.* 5(11):e15522.  
<http://dx.doi.org/10.1371/journal.pone.0015522>.
- Miltz W, Velcicky J, Dawson J, Littlewood-Evans A, Ludwig M-G, Seuwen K, Feifel R, Oberhauser B, Meyer A, Gabriel D, et al. 2017. Design and synthesis of potent and orally active GPR4 antagonists with modulatory effects on nociception, inflammation, and angiogenesis. *Bioorg Med Chem.* 25(16):4512–4525.  
<http://dx.doi.org/10.1016/j.bmc.2017.06.050>.
- Morgan JR, Prasad K, Jin S, Augustine GJ, Lafer EM. 2001. Uncoating of clathrin-coated vesicles in presynaptic terminals. *Neuron.* 32(2):289–300. [http://dx.doi.org/10.1016/s0896-6273\(01\)00467-6](http://dx.doi.org/10.1016/s0896-6273(01)00467-6).
- Murphy MP. 2009. How mitochondria produce reactive oxygen species. *Biochem J.* 417(1):1–13. <http://dx.doi.org/10.1042/BJ20081386>.
- Nakanishi K, Ida M, Suzuki H, Kitano C, Yamamoto A, Mori N, Araki M, Taketani S. 2006. Molecular characterization of a transport vesicle protein Neurensin-2, a homologue of Neurensin-1, expressed in neural cells. *Brain Res.* 1081(1):1–8.  
<http://dx.doi.org/10.1016/j.brainres.2006.01.085>.
- Narindrasorasak S, Kulkarni P, Deschamps P, She Y-M, Sarkar B. 2007. Characterization and copper binding properties of human COMMD1 (MURR1). *Biochemistry.* 46(11):3116–3128.  
<http://dx.doi.org/10.1021/bi0620656>.
- Ng CW, Yildirim F, Yap YS, Dalin S, Matthews BJ, Velez PJ, Labadorf A, Housman DE, Fraenkel E. 2013. Extensive changes in DNA methylation are associated with expression of mutant huntingtin. *Proc Natl Acad Sci U S A.* 110(6):2354–2359.  
<http://dx.doi.org/10.1073/pnas.1221292110>.

- Nicola SM, Surmeier J, Malenka RC. 2000. Dopaminergic modulation of neuronal excitability in the striatum and nucleus accumbens. *Annu Rev Neurosci.* 23(1):185–215. <http://dx.doi.org/10.1146/annurev.neuro.23.1.185>.
- Olgiati S, Quadri M, Fang M, Rood JPMA, Saute JA, Chien HF, Bouwkamp CG, Graafland J, Minneboo M, Breedveld GJ, et al. 2016. DNAJC6 mutations associated with early-onset Parkinson's disease: DNAJC6 mutations in Parkinson's disease. *Ann Neurol.* 79(2):244–256. <http://dx.doi.org/10.1002/ana.24553>.
- Pavlov AR, Revina AA, Dupin AM, Boldyrev AA, Yaropolov AI. 1993. The mechanism of interaction of carnosine with superoxide radicals in water solutions. *Biochim Biophys Acta Gen Subj.* 1157(2):304–312. [http://dx.doi.org/10.1016/0304-4165\(93\)90114-n](http://dx.doi.org/10.1016/0304-4165(93)90114-n).
- Paxinou E, Chen Q, Weisse M, Giasson BI, Norris EH, Rueter SM, Trojanowski JQ, Lee VM, Ischiropoulos H. 2001. Induction of alpha-synuclein aggregation by intracellular nitritive insult. *J Neurosci.* 21(20):8053–8061. <http://dx.doi.org/10.1523/jneurosci.21-20-08053.2001>.
- PD Med Collaborative Group, Gray R, Ives N, Rick C, Patel S, Gray A, Jenkinson C, McIntosh E, Wheatley K, Williams A, et al. 2014. Long-term effectiveness of dopamine agonists and monoamine oxidase B inhibitors compared with levodopa as initial treatment for Parkinson's disease (PD MED): a large, open-label, pragmatic randomised trial. *Lancet.* 384(9949):1196–1205. [http://dx.doi.org/10.1016/S0140-6736\(14\)60683-8](http://dx.doi.org/10.1016/S0140-6736(14)60683-8).
- Price R, Ferrari E, Gardoni F, Mercuri NB, Ledonne A. 2020. Protease-activated receptor 1 (PAR1) inhibits synaptic NMDARs in mouse nigral dopaminergic neurons. *Pharmacol Res.* 160(105185):105185. <http://dx.doi.org/10.1016/j.phrs.2020.105185>.
- Quan Y, Wang J, Wang S, Zhao J. 2020. Association of the plasma long non-coding RNA MEG3 with Parkinson's disease. *Front Neurol.* 11:532891. <http://dx.doi.org/10.3389/fneur.2020.532891>.
- Quinn PJ, Boldyrev AA, Formazuyk VE. 1992. Carnosine: its properties, functions and potential therapeutic applications. *Mol Aspects Med.* 13(5):379–444. [http://dx.doi.org/10.1016/0098-2997\(92\)90006-1](http://dx.doi.org/10.1016/0098-2997(92)90006-1).
- Qureshi IA, Mehler MF. 2011. Advances in epigenetics and epigenomics for neurodegenerative diseases. *Curr Neurol Neurosci Rep.* 11(5):464–473. <http://dx.doi.org/10.1007/s11910-011-0210-2>.
- Roosen DA, Blauwendraat C, Cookson MR, Lewis PA. 2019. DNAJC proteins and pathways to parkinsonism. *FEBS J.* 286(16):3080–3094. <http://dx.doi.org/10.1111/febs.14936>.
- Ru F, Banovcin P Jr, Kollarik M. 2015. Acid sensitivity of the spinal dorsal root ganglia C-fiber nociceptors innervating the guinea pig esophagus. *Neurogastroenterol Motil.* 27(6):865–874. <http://dx.doi.org/10.1111/nmo.12561>.
- Rudinskiy N, Kaneko YA, Beesen AA, Gokce O, Régulier E, Déglon N, Luthi-Carter R. 2009. Diminished hippocalcin expression in Huntington's disease brain does not account for increased striatal neuron vulnerability as assessed in primary neurons. *J Neurochem.* 111(2):460–472. <http://dx.doi.org/10.1111/j.1471-4159.2009.06344.x>.

- Scudamore O, Ciossek T. 2018. Increased oxidative stress exacerbates  $\alpha$ -synuclein aggregation in vivo. *J Neuropathol Exp Neurol*. 77(6):443–453. <http://dx.doi.org/10.1093/jnen/nly024>.
- Shen R-S, Abell CW, Gessner W, Bossi A. 1985. Serotonergic conversion of MPTP and dopaminergic accumulation of MPP<sup>+</sup>. *FEBS Lett*. 189(2):225–230. [http://dx.doi.org/10.1016/0014-5793\(85\)81028-0](http://dx.doi.org/10.1016/0014-5793(85)81028-0).
- Sherer TB, Kim J-H, Betarbet R, Greenamyre JT. 2003. Subcutaneous rotenone exposure causes highly selective dopaminergic degeneration and  $\alpha$ -synuclein aggregation. *Exp Neurol*. 179(1):9–16. <http://dx.doi.org/10.1006/exnr.2002.8072>.
- Shihan MH, Novo SG, Le Marchand SJ, Wang Y, Duncan MK. 2021. A simple method for quantitating confocal fluorescent images. *Biochem Biophys Rep*. 25(100916):100916. <http://dx.doi.org/10.1016/j.bbrep.2021.100916>.
- Spillantini MG, Crowther RA, Jakes R, Hasegawa M, Goedert M. 1998.  $\alpha$ -Synuclein in filamentous inclusions of Lewy bodies from Parkinson's disease and dementia with Lewy bodies. *Proc Natl Acad Sci U S A*. 95(11):6469–6473. <http://dx.doi.org/10.1073/pnas.95.11.6469>.
- Stetler RA, Gan Y, Zhang W, Liou AK, Gao Y, Cao G, Chen J. 2010. Heat shock proteins: cellular and molecular mechanisms in the central nervous system. *Prog Neurobiol*. 92(2):184–211. <http://dx.doi.org/10.1016/j.pneurobio.2010.05.002>.
- Stocchi F, Borgohain R, Onofrij M, Schapira AHV, Bhatt M, Lucini V, Giuliani R, Anand R, Study 015 Investigators. 2012. A randomized, double-blind, placebo-controlled trial of safinamide as add-on therapy in early Parkinson's disease patients: Safinamide as ADD-ON Therapy in Early PD. *Mov Disord*. 27(1):106–112. <http://dx.doi.org/10.1002/mds.23954>.
- Stocchi F, Olanow CW. 2013. Obstacles to the development of a neuroprotective therapy for Parkinson's disease: Obstacles to neuroprotection. *Mov Disord*. 28(1):3–7. <http://dx.doi.org/10.1002/mds.25337>.
- Stockwell PA, Chatterjee A, Rodger EJ, Morison IM. 2014. DMAP: differential methylation analysis package for RRBS and WGBS data. *Bioinformatics*. 30(13):1814–1822. <http://dx.doi.org/10.1093/bioinformatics/btu126>.
- Stvolinskii SL, Fedorova TN, Yuneva MO, Boldyrev AA. 2003. Protective effect of carnosine on Cu,Zn-superoxide dismutase during impaired oxidative metabolism in the brain in vivo. *Bull Exp Biol Med*. 135(2):130–132. <http://dx.doi.org/10.1023/a:1023855428130>.
- Teuscher NS, Shen H, Shu C, Xiang J, Keep RF, Smith DE. 2004. Carnosine uptake in rat choroid plexus primary cell cultures and choroid plexus whole tissue from PEPT2 null mice. *J Neurochem*. 89(2):375–382. <http://dx.doi.org/10.1111/j.1471-4159.2004.02333.x>.
- Umeda A, Meyerholz A, Ungewickell E. 2000. Identification of the universal cofactor (auxilin 2) in clathrin coat dissociation. *Eur J Cell Biol*. 79(5):336–342. [http://dx.doi.org/10.1078/S0171-9335\(04\)70037-0](http://dx.doi.org/10.1078/S0171-9335(04)70037-0).
- Umschweif G, Medrihan L, Guillén-Samander A, Wang W, Sagi Y, Greengard P. 2021. Identification of Neurensin-2 as a novel modulator of emotional behavior. *Mol Psychiatry*. 26(7):2872–2885. <http://dx.doi.org/10.1038/s41380-021-01058-5>.

- Valente EM, Abou-Sleiman PM, Caputo V, Muqit MMK, Harvey K, Gispert S, Ali Z, Del Turco D, Bentivoglio AR, Healy DG, et al. 2004. Hereditary early-onset Parkinson's disease caused by mutations in PINK1. *Science*. 304(5674):1158–1160. <http://dx.doi.org/10.1126/science.1096284>.
- Velcicky J, Miltz W, Oberhauser B, Orain D, Vaupel A, Weigand K, Dawson King J, Littlewood-Evans A, Nash M, Feifel R, et al. 2017. Development of selective, orally active GPR4 antagonists with modulatory effects on nociception, inflammation, and angiogenesis. *J Med Chem*. 60(9):3672–3683. <http://dx.doi.org/10.1021/acs.jmedchem.6b01703>.
- Vidović M, Rikalovic MG. 2022. Alpha-synuclein aggregation pathway in Parkinson's disease: Current status and novel therapeutic approaches. *Cells*. 11(11):1732. <http://dx.doi.org/10.3390/cells11111732>.
- Voigt JM, Guengerich FP, Baron J. 1993. Localization and induction of cytochrome P450 1A1 and aryl hydrocarbon hydroxylase activity in rat nasal mucosa. *J Histochem Cytochem*. 41(6):877–885. <http://dx.doi.org/10.1177/41.6.8315279>.
- Vonk WIM, Bartuzi P, de Bie P, Kloosterhuis N, Wichers CGK, Berger R, Haywood S, Klomp LWJ, Wijmenga C, van de Sluis B. 2011. Liver-specific Commd1 knockout mice are susceptible to hepatic copper accumulation. *PLoS One*. 6(12):e29183. <http://dx.doi.org/10.1371/journal.pone.0029183>.
- Vonk WIM, de Bie P, Wichers CGK, van den Berghe PVE, van der Plaats R, Berger R, Wijmenga C, Klomp LWJ, van de Sluis B. 2012. The copper-transporting capacity of ATP7A mutants associated with Menkes disease is ameliorated by COMMD1 as a result of improved protein expression. *Cell Mol Life Sci*. 69(1):149–163. <http://dx.doi.org/10.1007/s00018-011-0743-1>.
- Vonk WIM, Kakkar V, Bartuzi P, Jaarsma D, Berger R, Hofker MH, Klomp LWJ, Wijmenga C, Kampinga HH, van de Sluis B. 2014. The Copper Metabolism MURR1 domain protein 1 (COMMD1) modulates the aggregation of misfolded protein species in a client-specific manner. *PLoS One*. 9(4):e92408. <http://dx.doi.org/10.1371/journal.pone.0092408>.
- Wallace DC, Fan W, Procaccio V. 2010. Mitochondrial energetics and therapeutics. *Annu Rev Pathol*. 5:297–348. <http://dx.doi.org/10.1146/annurev.pathol.4.110807.092314>.
- Wang Y, de Vallière C, Imenez Silva PH, Leonardi I, Gruber S, Gerstgrasser A, Melhem H, Weber A, Leucht K, Wolfram L, et al. 2018. The proton-activated receptor GPR4 modulates intestinal inflammation. *J Crohns Colitis*. 12(3):355–368. <http://dx.doi.org/10.1093/ecco-jcc/jjx147>.
- Wen T, Qu F, Li NB, Luo HQ. 2017. A facile, sensitive, and rapid spectrophotometric method for copper(II) ion detection in aqueous media using polyethyleneimine. *Arab J Chem*. 10:S1680–S1685. <http://dx.doi.org/10.1016/j.arabjc.2013.06.013>.
- Winklhofer KF, Haass C. 2010. Mitochondrial dysfunction in Parkinson's disease. *Biochim Biophys Acta*. 1802(1):29–44. <http://dx.doi.org/10.1016/j.bbadis.2009.08.013>.

- Wooten GF, Currie LJ, Bovbjerg VE, Lee JK, Patrie J. 2004. Are men at greater risk for Parkinson's disease than women? *J Neurol Neurosurg Psychiatry*. 75(4):637–639. <http://dx.doi.org/10.1136/jnnp.2003.020982>.
- Yu M, Cui R, Huang Y, Luo Y, Qin S, Zhong M. 2019. Increased proton-sensing receptor GPR4 signalling promotes colorectal cancer progression by activating the hippo pathway. *EBioMedicine*. 48:264–276. <http://dx.doi.org/10.1016/j.ebiom.2019.09.016>.
- Zhou Q, Li J, Wang H, Yin Y, Zhou J. 2011. Identification of nigral dopaminergic neuron-enriched genes in adult rats. *Neurobiol Aging*. 32(2):313–326. <http://dx.doi.org/10.1016/j.neurobiolaging.2009.02.009>.
- Zhu M, Xing D, Lu Z, Fan Y, Hou W, Dong Hailong, Xiong L, Dong Hui. 2015. DDR1 may play a key role in destruction of the blood-brain barrier after cerebral ischemia-reperfusion. *Neurosci Res*. 96:14–19. <http://dx.doi.org/10.1016/j.neures.2015.01.004>.
- Zhu W, Xie W, Pan T, Jankovic J, Li J, Youdim MBH, Le W. 2008. Comparison of neuroprotective and neurorestorative capabilities of rasagiline and selegiline against lactacystin-induced nigrostriatal dopaminergic degeneration. *J Neurochem*. 105(5):1970–1978. <http://dx.doi.org/10.1111/j.1471-4159.2008.05330.x>.